AURORA: GLOBAL FEATURES

Jean-Claude Gérard
LPAP – Université de Liège

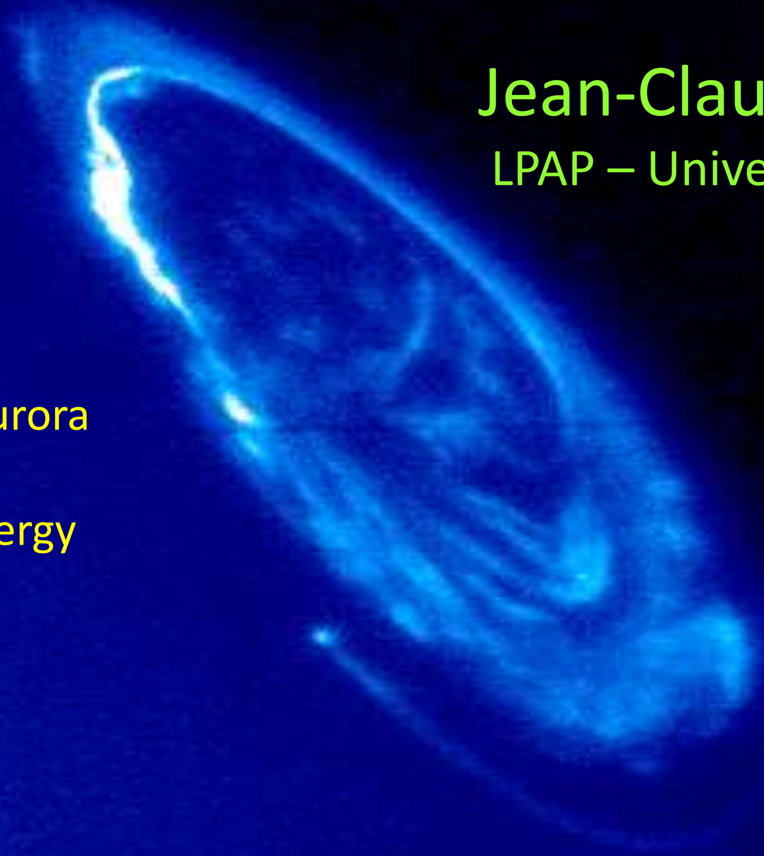

OUTLINE

- collisional processes involved in the aurora

- remote sensing of auroral electron energy

- Jupiter

- Saturn

MOP meeting - 2011

July 14, 2011

1. Collisional processes

involved in the aurora

$$e_p + H_2 \rightarrow H_2^* \,(B, C, B', C', \ldots) + e$$

These inelastic collision processes compete with ionization:

$$e_p + H_2 \rightarrow H_2^+ + e_p + e_s$$

These secondary electrons can in turn collide and excite H_2 levels

$$e_s + H_2 \rightarrow H_2^* \,(B, C, B', C', D, \ldots) + e_s$$

- The bulk of the UV excitation is caused by the secondary electrons
- The FUV and EUV emission from H_2^* is instantaneous and directly reflects the morphology and intensity of the electron precipitation.

Efficiency of the Ultraviolet H_2 emission

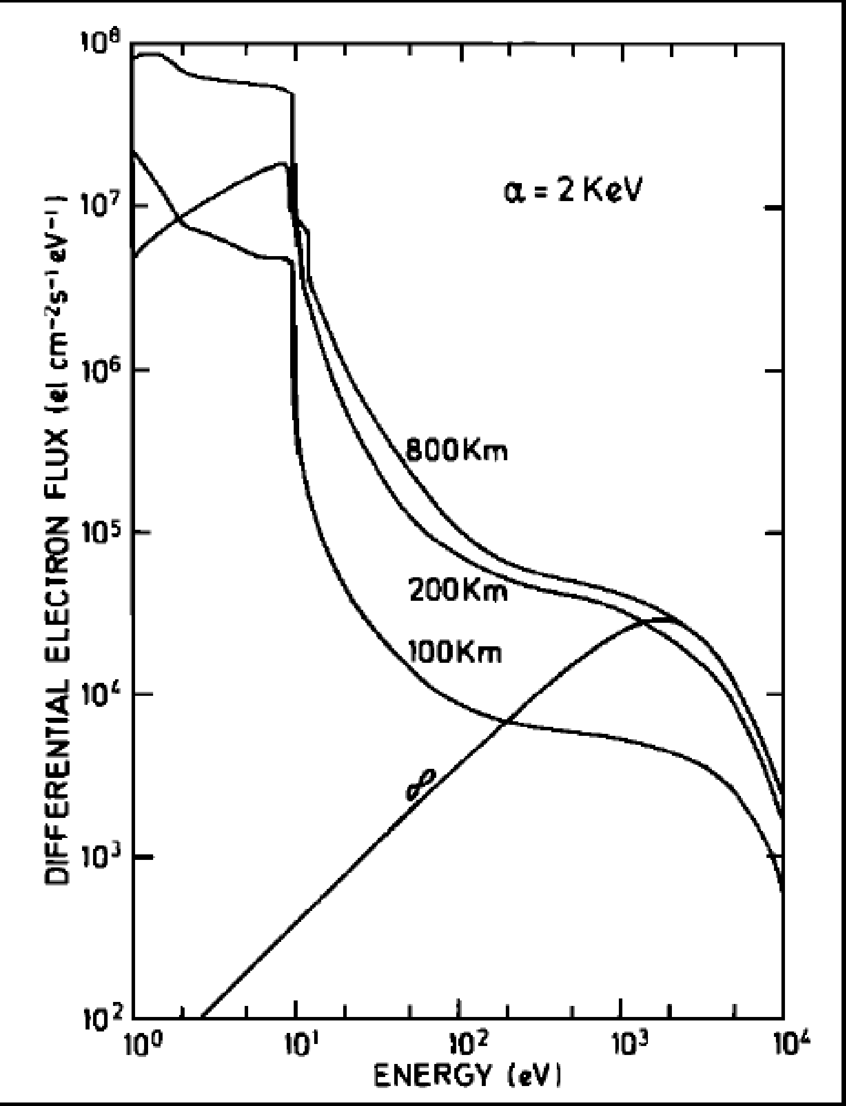

For e^- precipitation with a mean energy exceeding a few hundred eV:

H_2 emission in the Lyman (B-X) and Werner (C-X) bands:

Waite et al. (1983): $\varepsilon = 9.2$ kR/mW m^{-2}

Gérard & Singh (1982): $\varepsilon = 10.6$ kR / mW m^{-2}

Grodent et al. (2002): $\varepsilon = 10$ kR/mW m^{-2}

Partitioning between FUV and EUV

- The H_2 emission spectrum covers the range 72-185 nm
- The fractions below (EUV) and above (FUV) Lyman-α are 50.3 and 49.7 %
- The Lyman (B state) and Werner (C state) emissions amount to 90.4 % of the total H_2 emission

Ultraviolet and infrared aurora

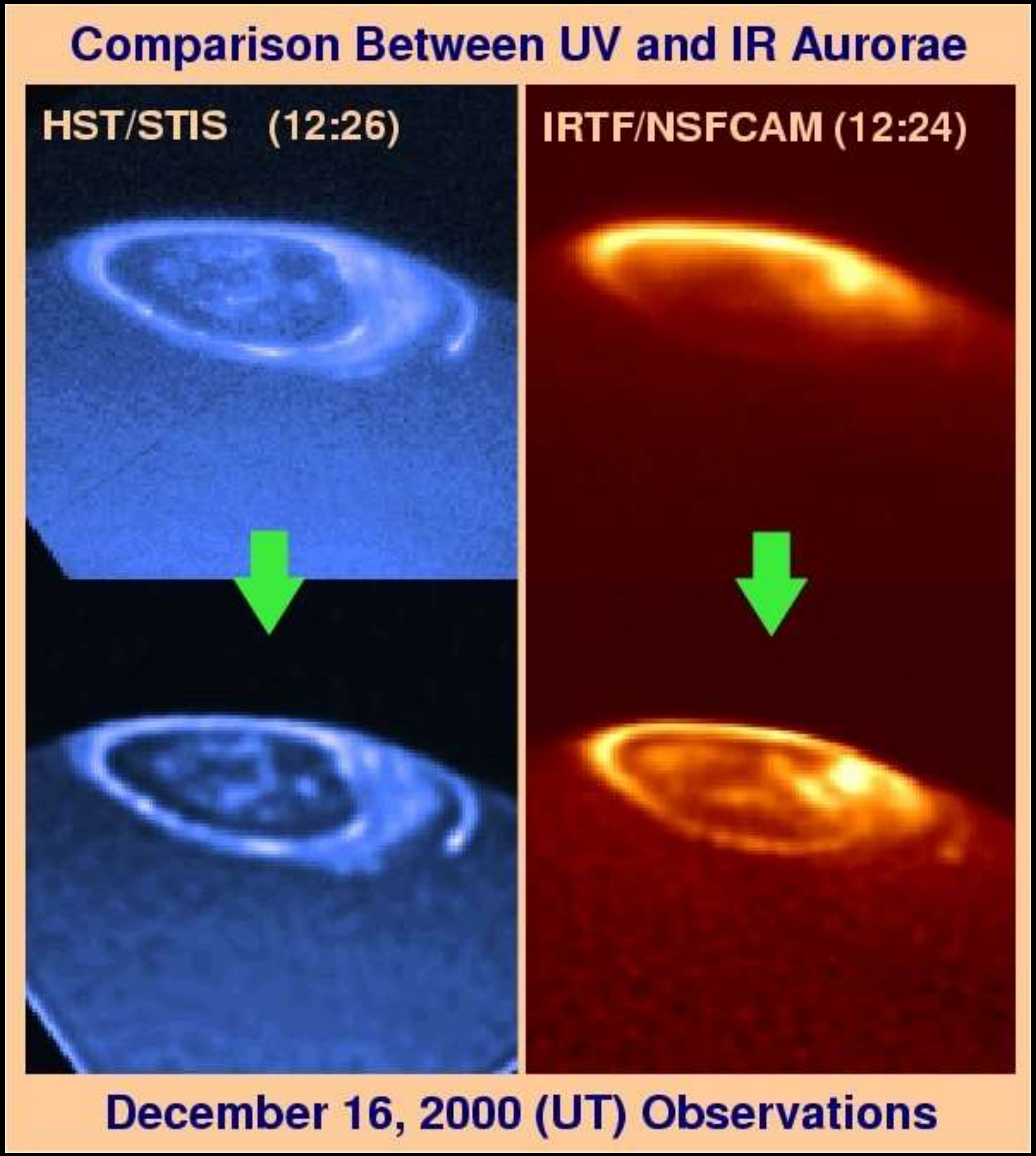

Clarke et al., 20xx

Most morphological features are similar, but differences are observed in the relative intensity of different features.

$$H_2 + H_2^+ \rightarrow H_3^+ + H$$

is the source of the infrared aurora

The H_3^+ emission reflects both the H_3^+ density and the population of excited H_3^+ which depends on the local temperature.

Consequently:

-the IR aurora is not a direct image of the morphology of the total electron energy flux

- its intensity is not linear with the precipitated energy flux

- a timelag is involved between the formation of the H_2^+ ion and the IR photon emission because the lifetime of H_3^+ ions may be as long as 100-1000 seconds

2. Remote sensing of the energy of auroral electrons

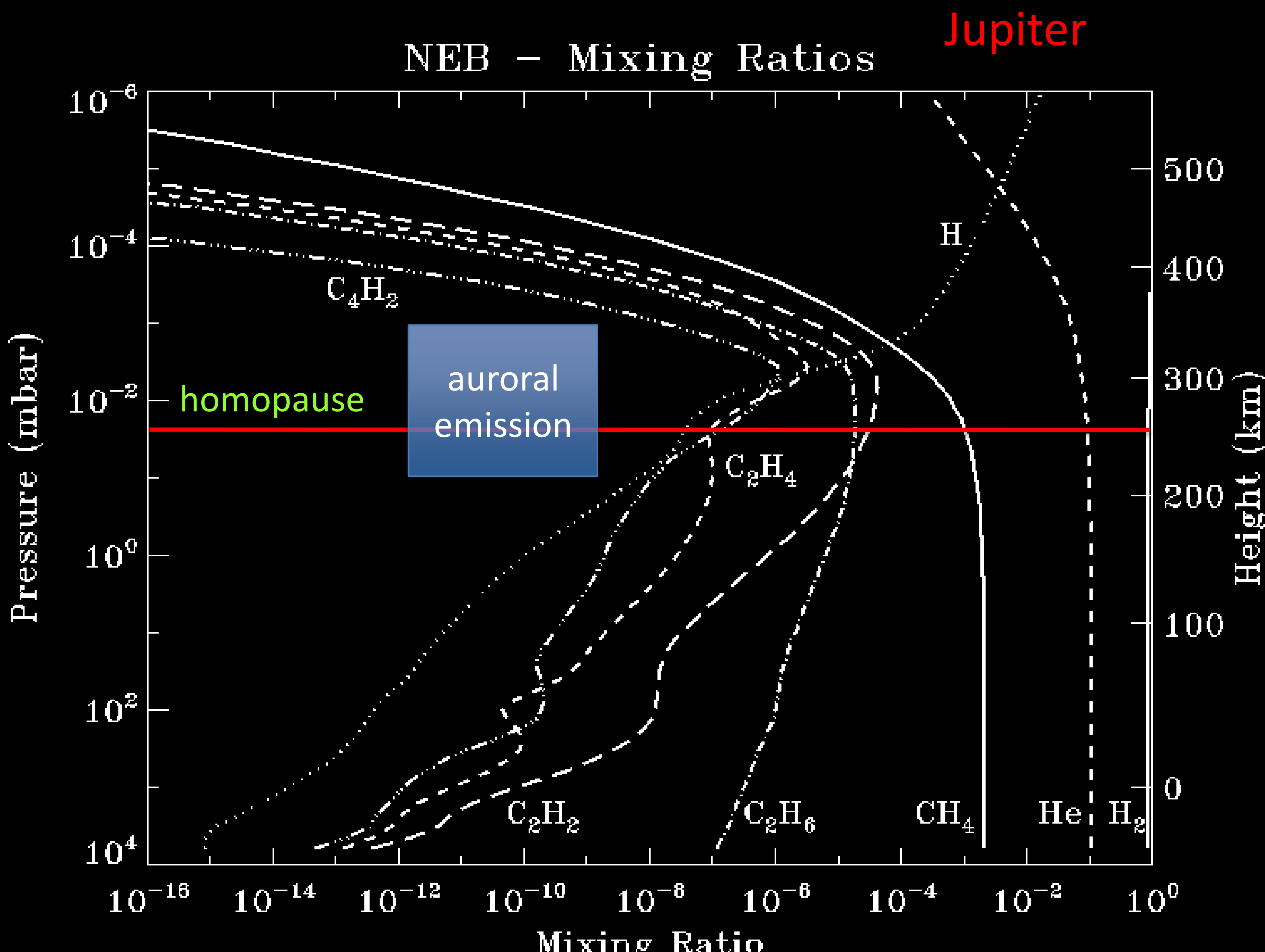
Jupiter
NEB – Mixing Ratios
Pressure (mbar)
Height (km)
Mixing Ratio
homopause
auroral emission
C_4H_2
C_2H_4
C_2H_2
C_2H_6
CH_4
He
H_2
H
10^{-6}
10^{-4}
10^{-2}
10^{0}
10^{2}
10^{4}
500
400
300
200
100
0
10^{-16}
10^{-14}
10^{-12}
10^{-10}
10^{-8}
10^{-6}
10^{-4}
10^{-2}
10^{0}

FUV Color ratio

The FUV color ratio may thus be used to determine the characteristic energy of auroral precipitation in giant planets' atmospheres if the vertical distribution of hydrocarbons is known.

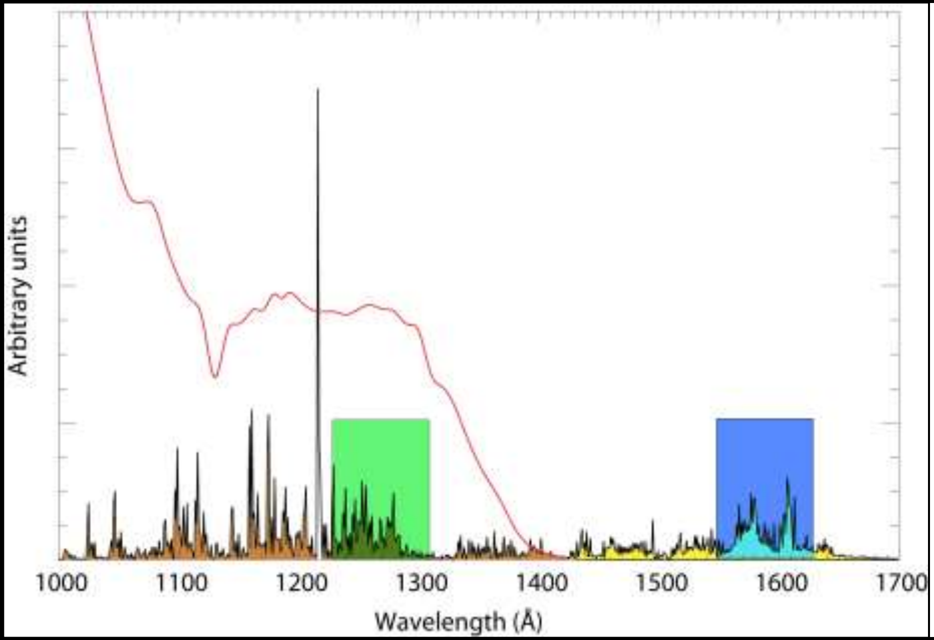

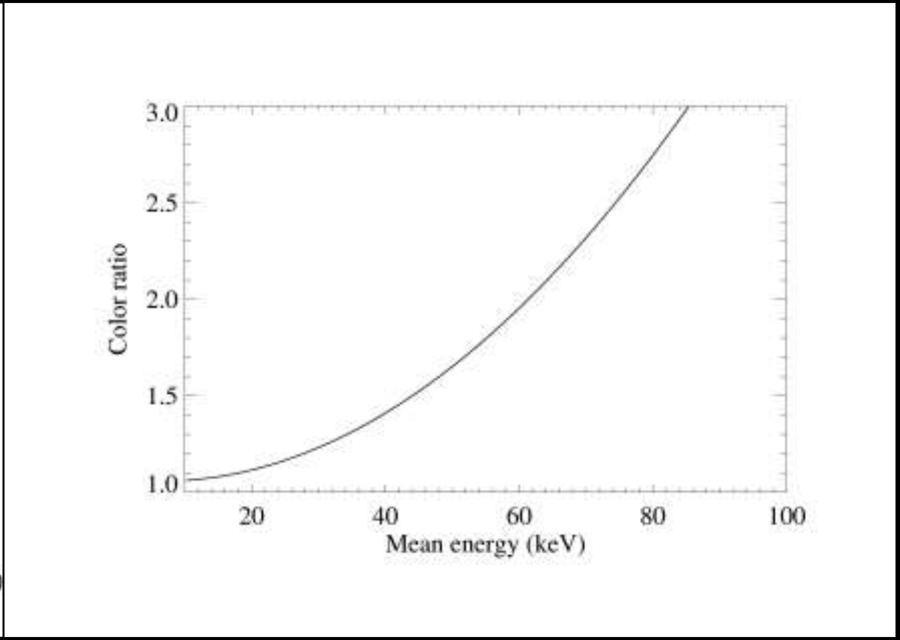

The FUV color ratio (CR) $\dfrac{I(1550 - 1620\,\text{Å})}{I(1230 - 1300\,\text{Å})}$

Unabsorbed value: 1.1

Latitudinal cut along the STIS slit (Jupiter)

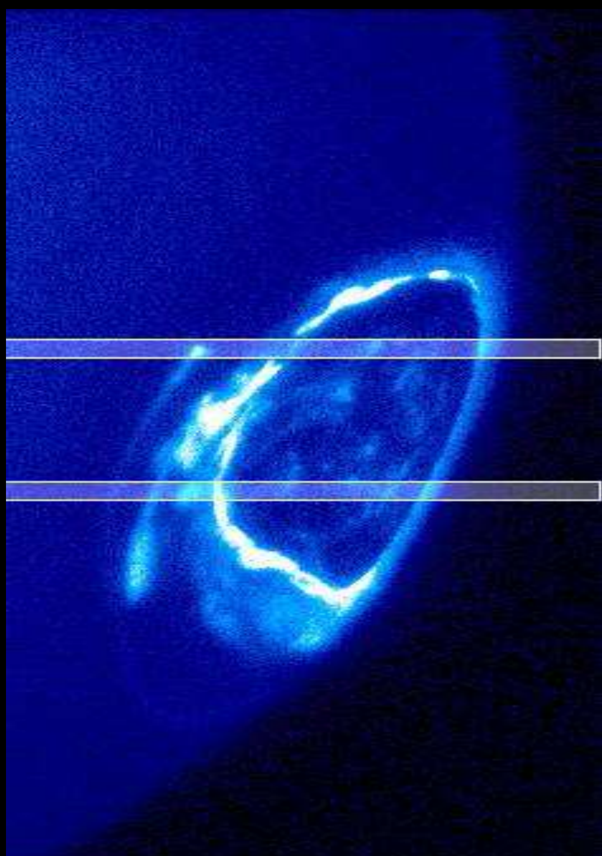

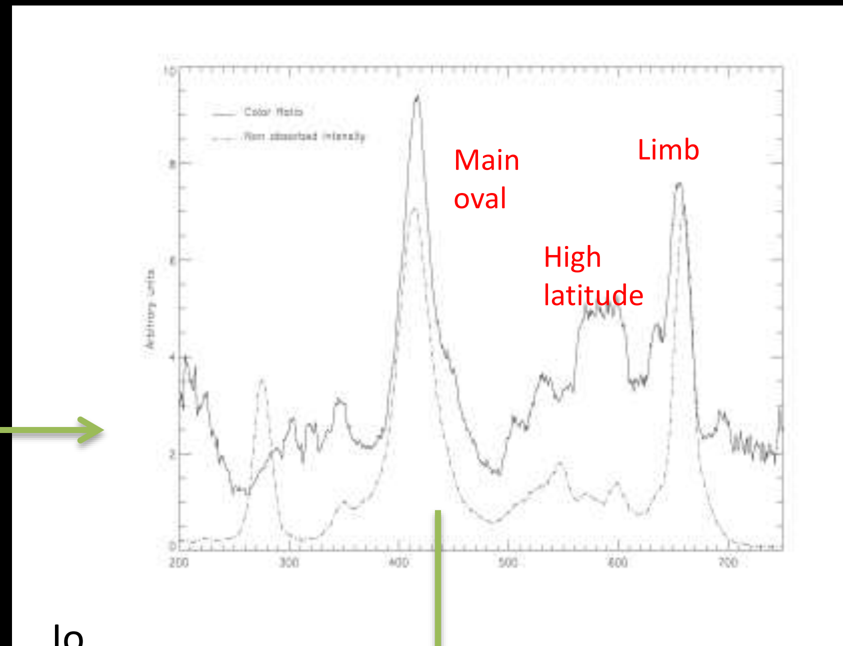

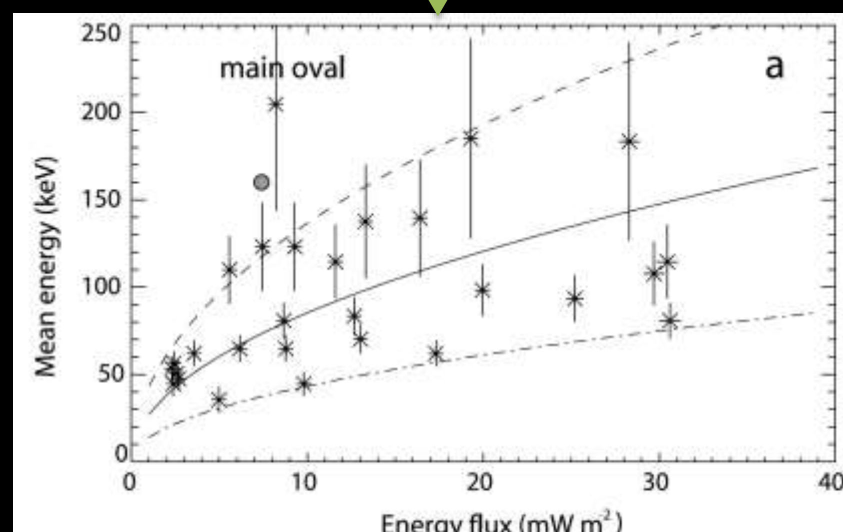

3. Jupiter's aurora

The complexity of the Jovian aurora

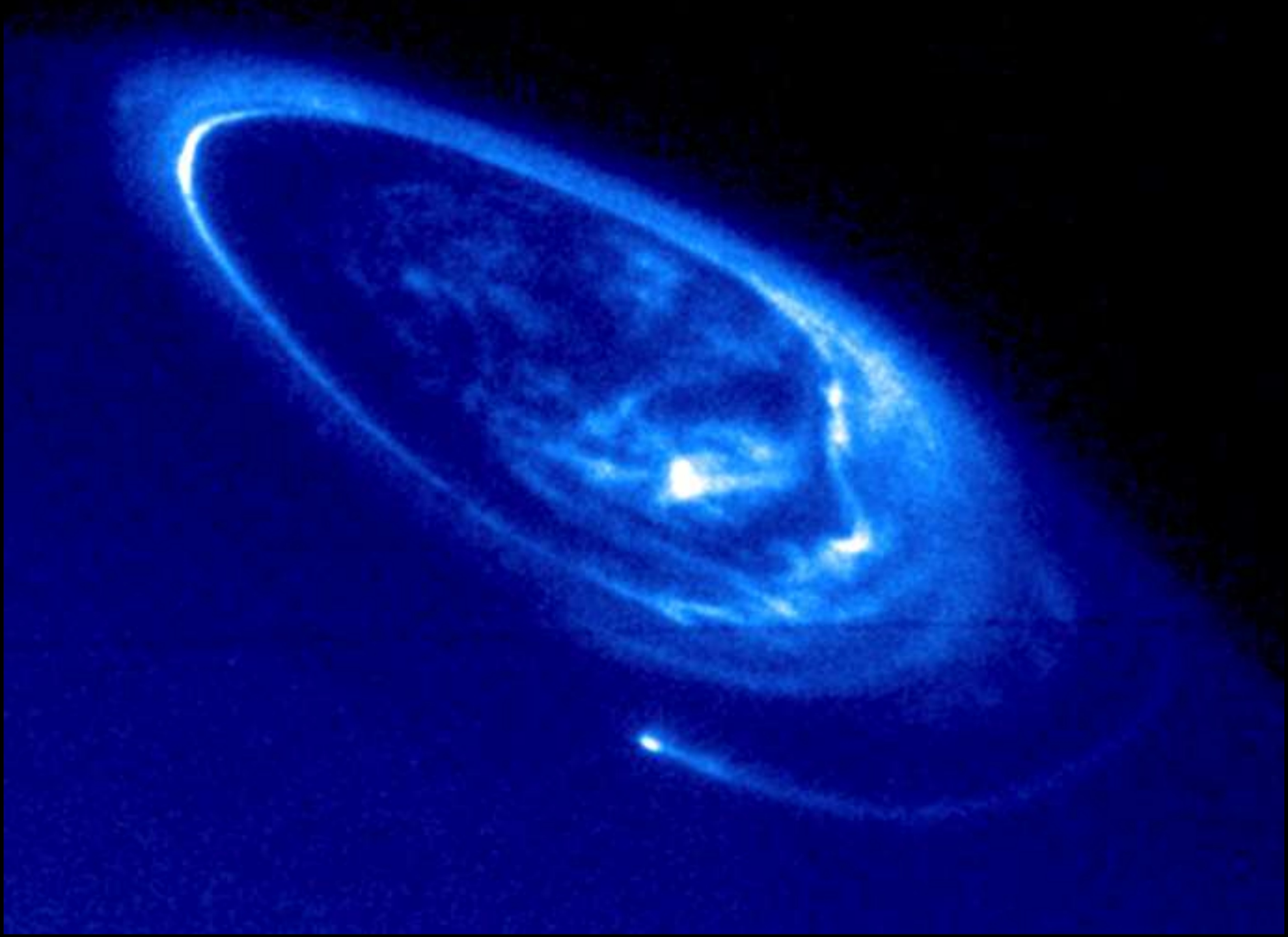

The complexity of the Jovian aurora

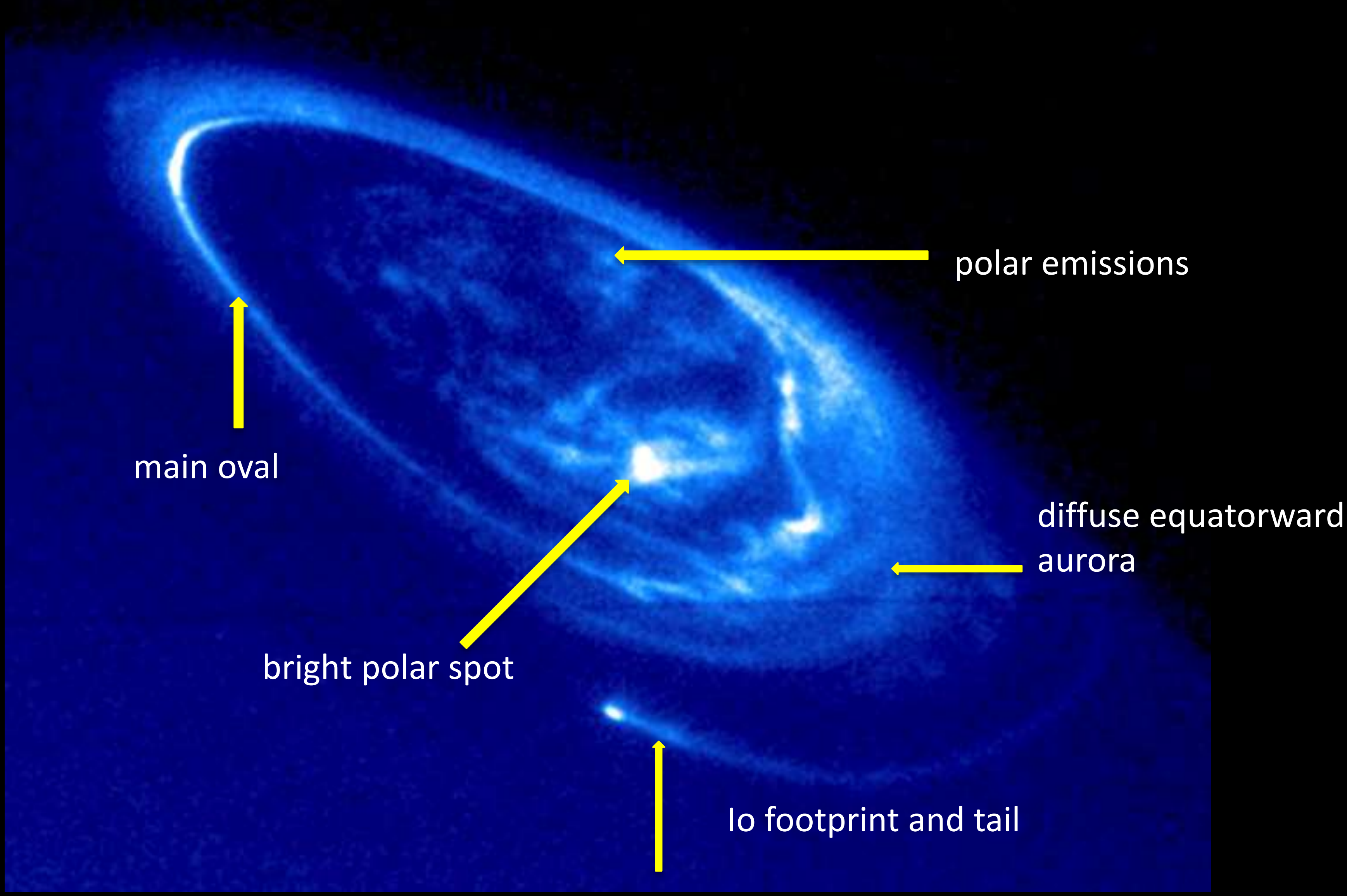

Equatorward diffuse emissions (EDEs)

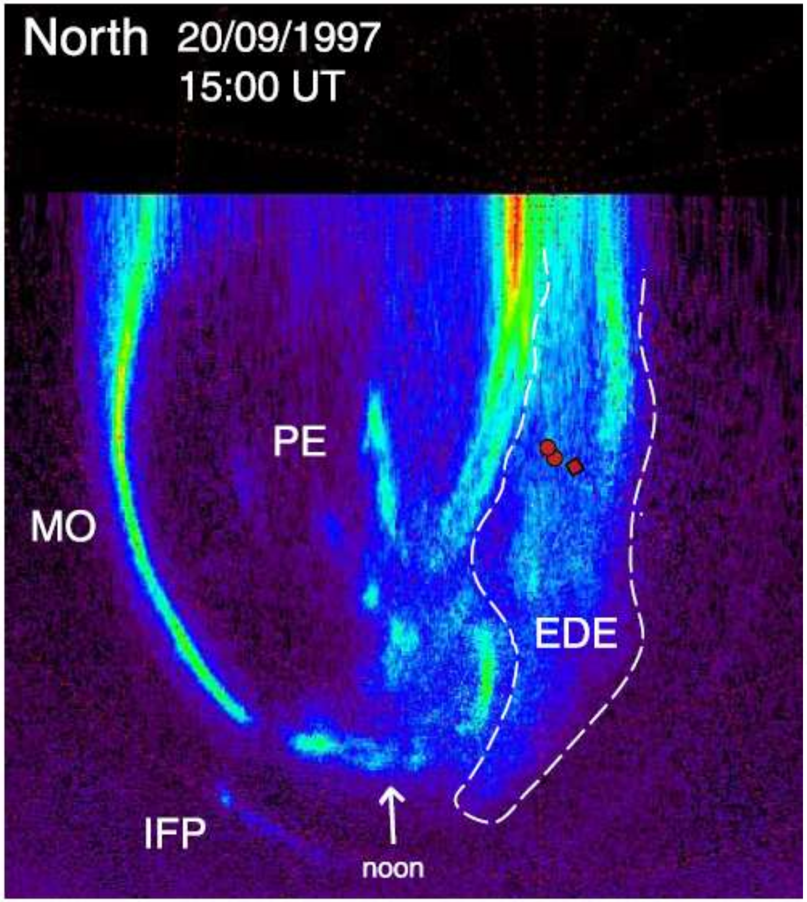

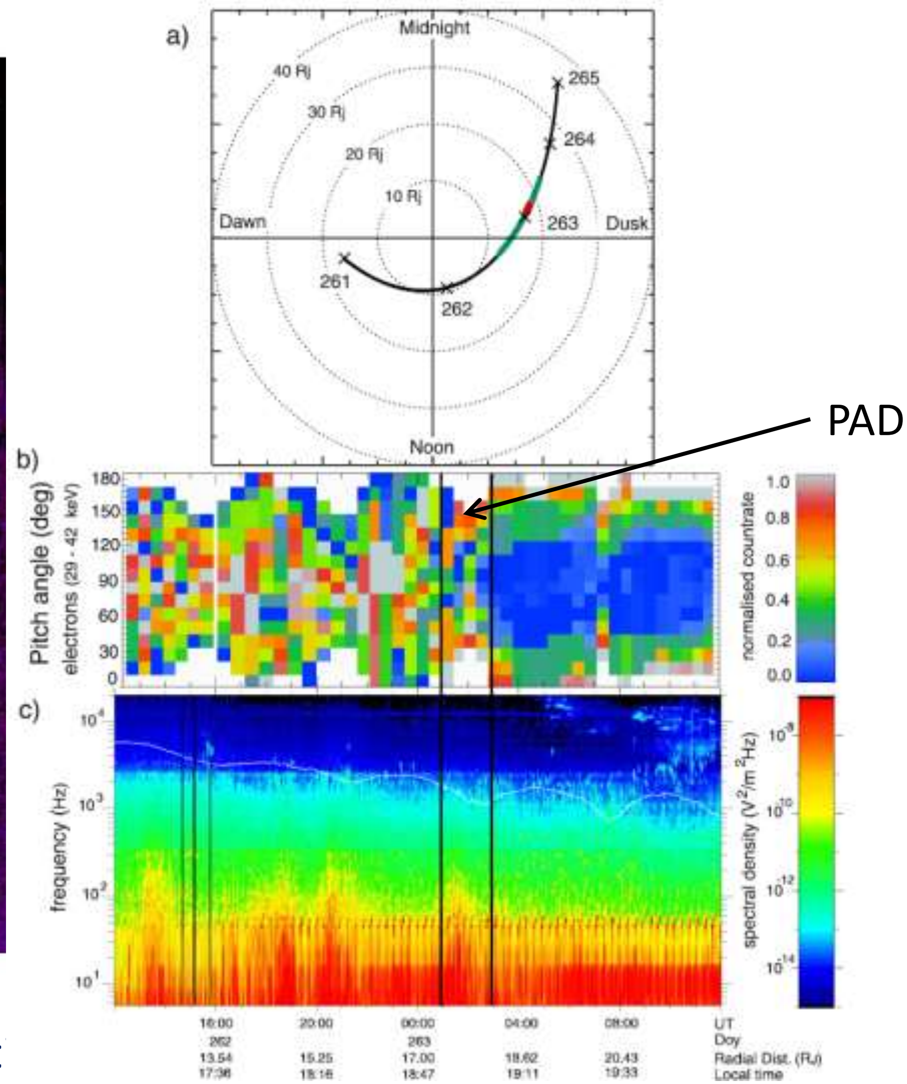

The red dots indicate the mapped locat
boundary observed by Galileo on the same day at 01:00 – 03:00 UT

Radioti et al., 2009

Polar dawn spots and nightside spots

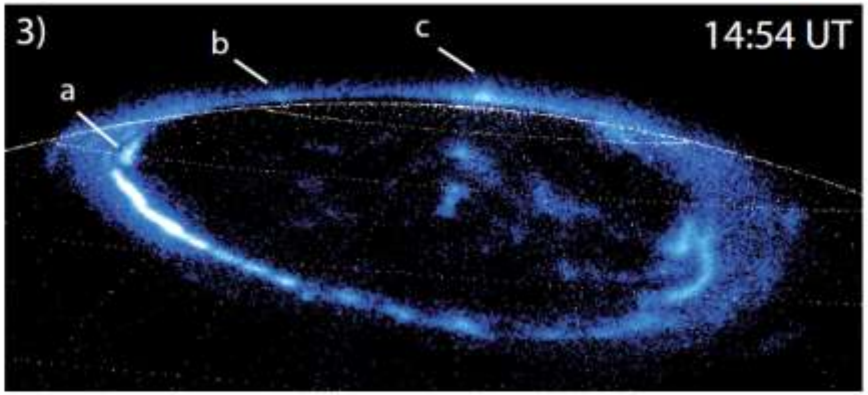

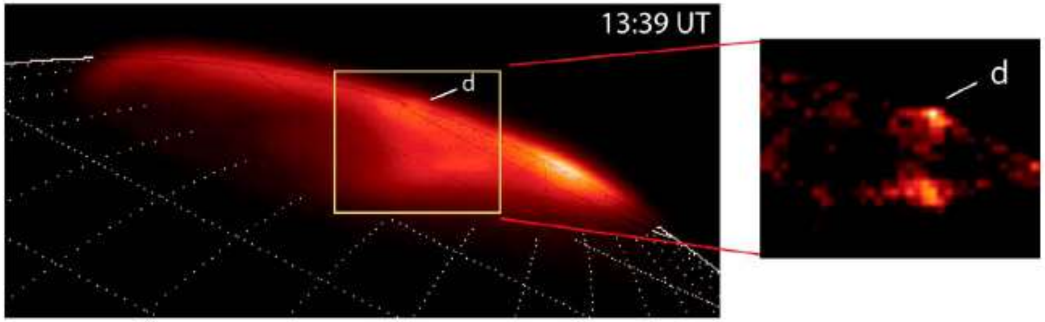

location of the spots in the equatorial plane

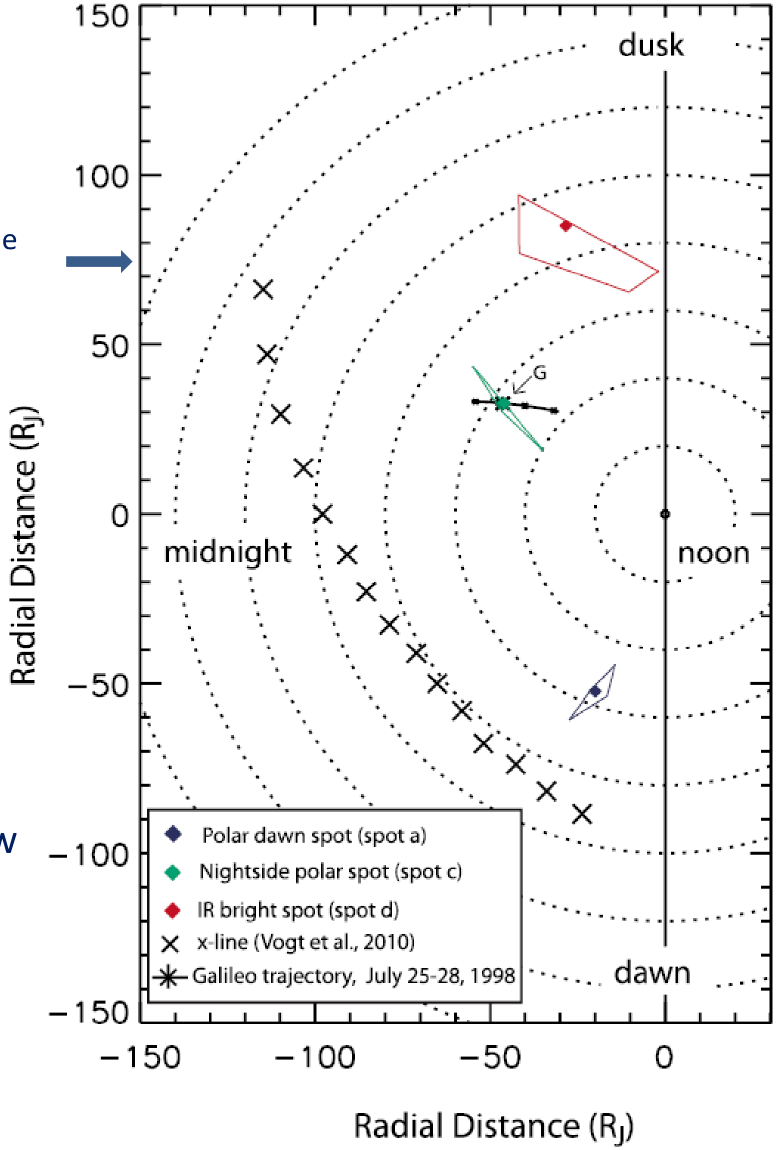

- On the same day Galileo observed an inward moving flow released during tail reconnection close to the mapped location of spot b supporting an association of the polar spot with tail dynamics.
- Observations indicate that the transient nightside spots could have a common origin: tail reconnection as shown in previous studies for the UV spots (Radioti et al., 2010)

Radioti et al., 2011

Auroral pulsations at high southern latitudes

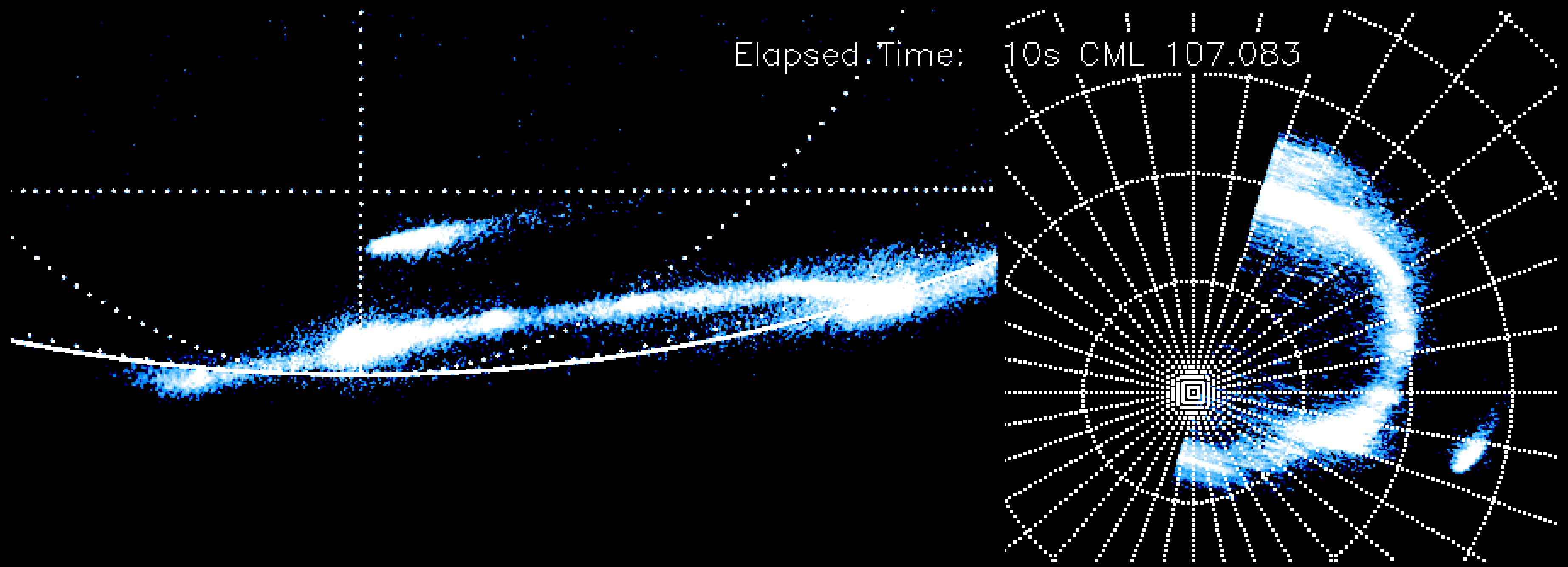

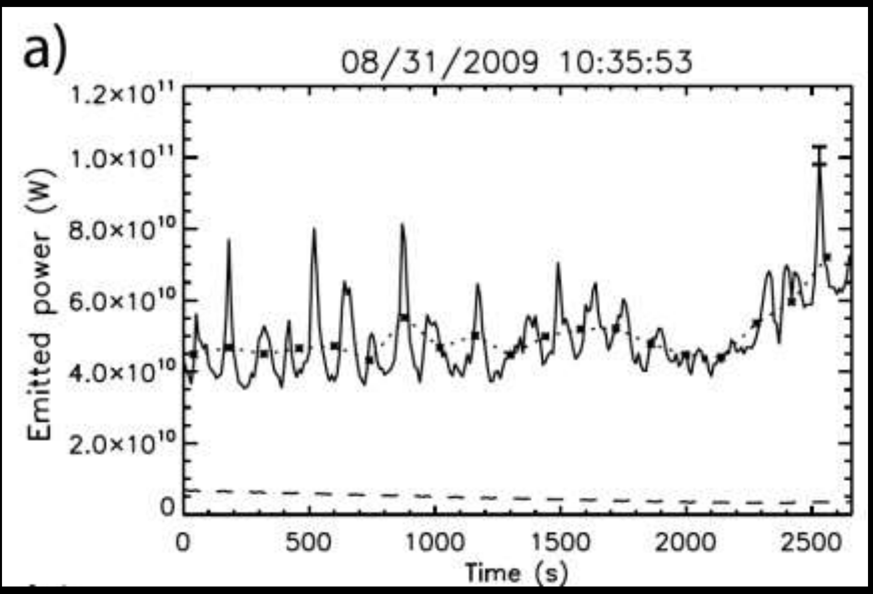

period: 2-3 min.
excess power: 10-40 GW
magnetic mapping: 55 to 120 R_J
10:00 to 18:00 LT

Bonfond et al., 2011

Size of the Io and Ganymede footprints

- The Io footprint width is <200 km to match the observations
- Interaction region: Io's close neighborhood

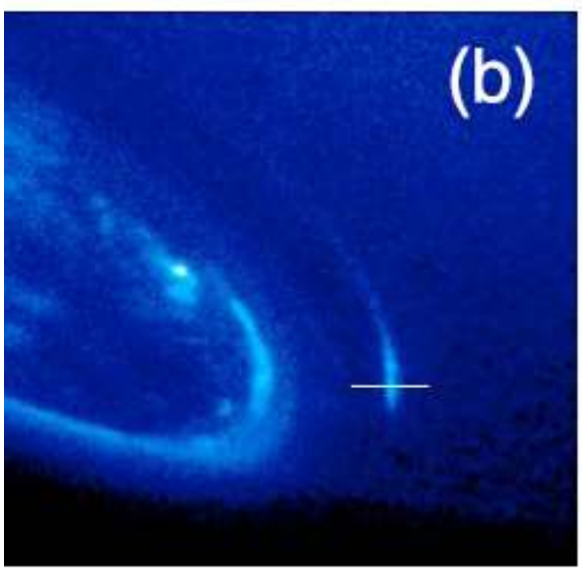

Bonfond , 2010

- The Ganymede footprint maps to a characteristic diameter of 8-20 R_G
- Interaction region: the whole Ganymede magnetosphere

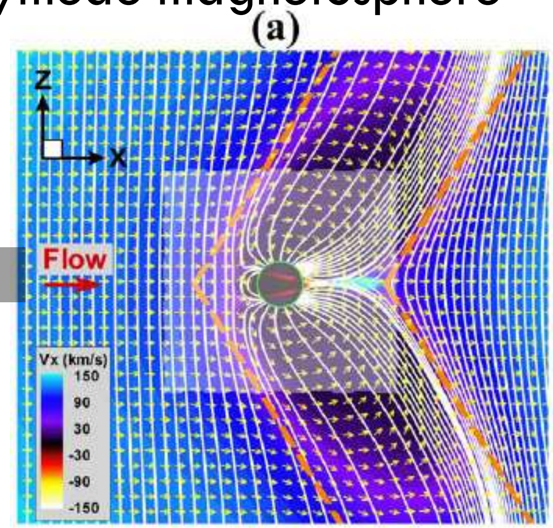

Jia et al., 2009

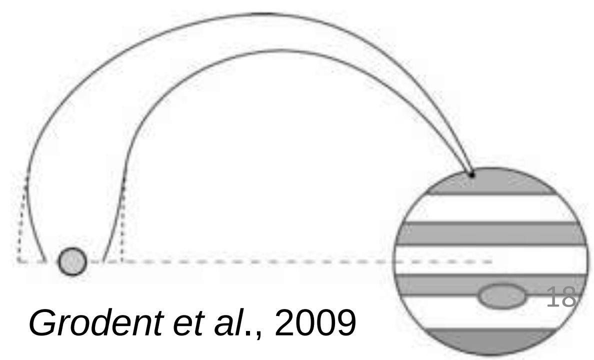

Grodent et al., 2009

4. Saturn’s aurora

The complexity of Saturn's aurora

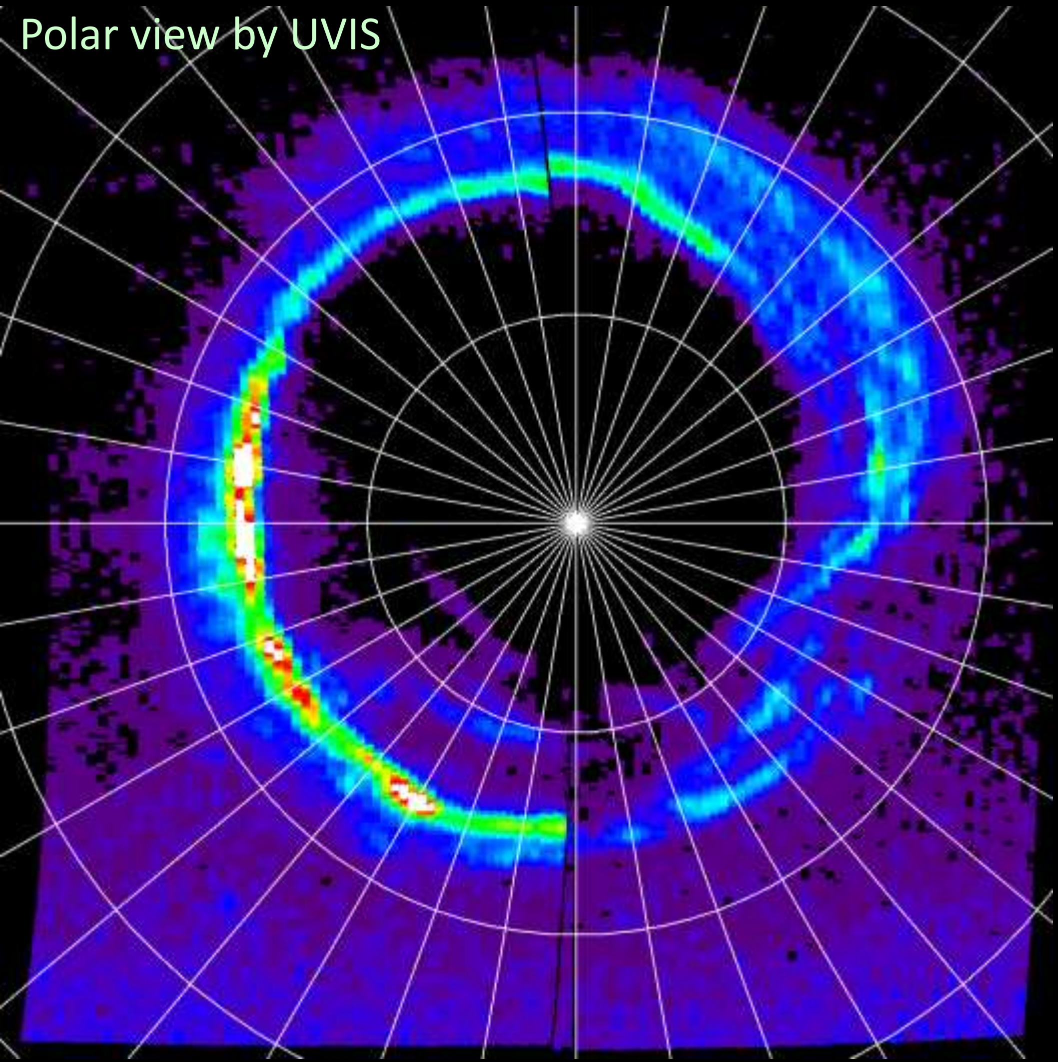

Grodent et al., in press

The main auroral emission appears associated with the open-closed field line boundary.
However, the structure is complex, showing:

Secondary oval
Diffuse emission
Bifurcations
Spirals
Cusp signature

In addition, asymmetries are observed between the two polar regions:

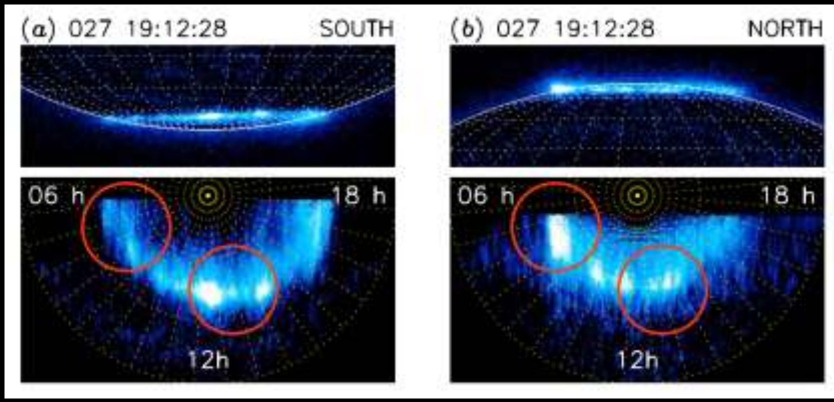

Nichols et al., 2009

BIFURCATIONS: reconnection at Saturn's magnetopause

The bifurcations can be related to reconnection at the flank of the magnetopause

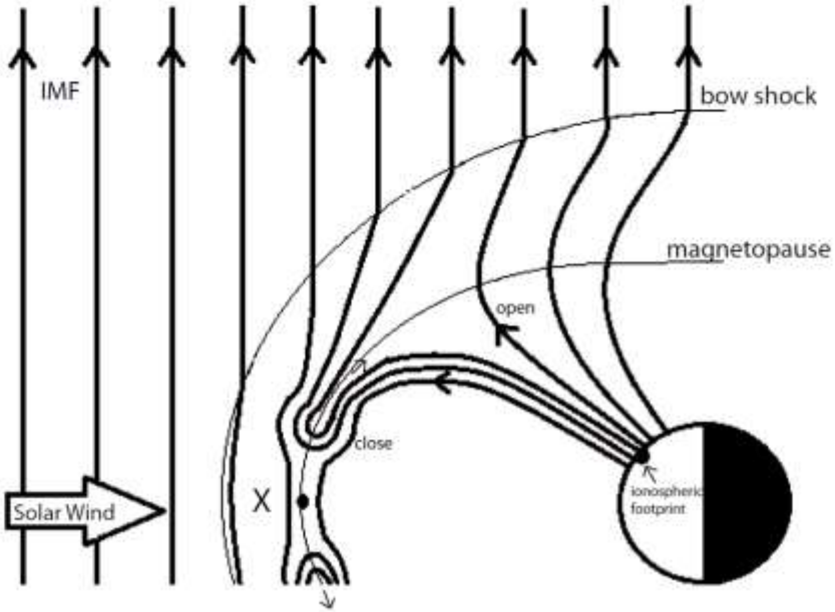

Adapted from Lockwood and Wild (1993)

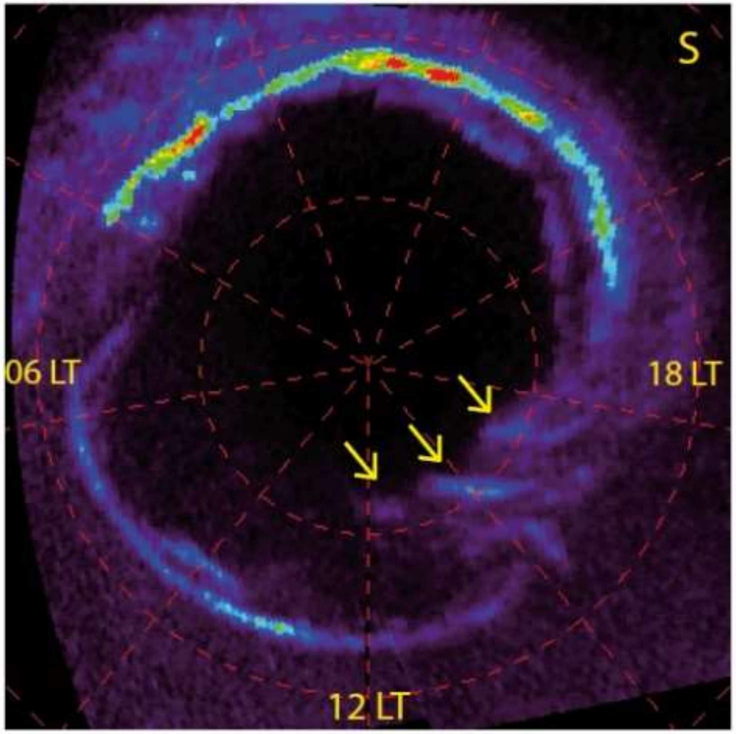

- Closed field lines are converted to open.
- A pair of bubbles of mixed magnetospheric and magnetosheath plasma is produced and moved away from the X point.
- Cassini observations revealed signatures of reconnection at Saturn's magnetopause (McAndrews et al., 2008)

Radioti et al., submitted

Enceladus footprint

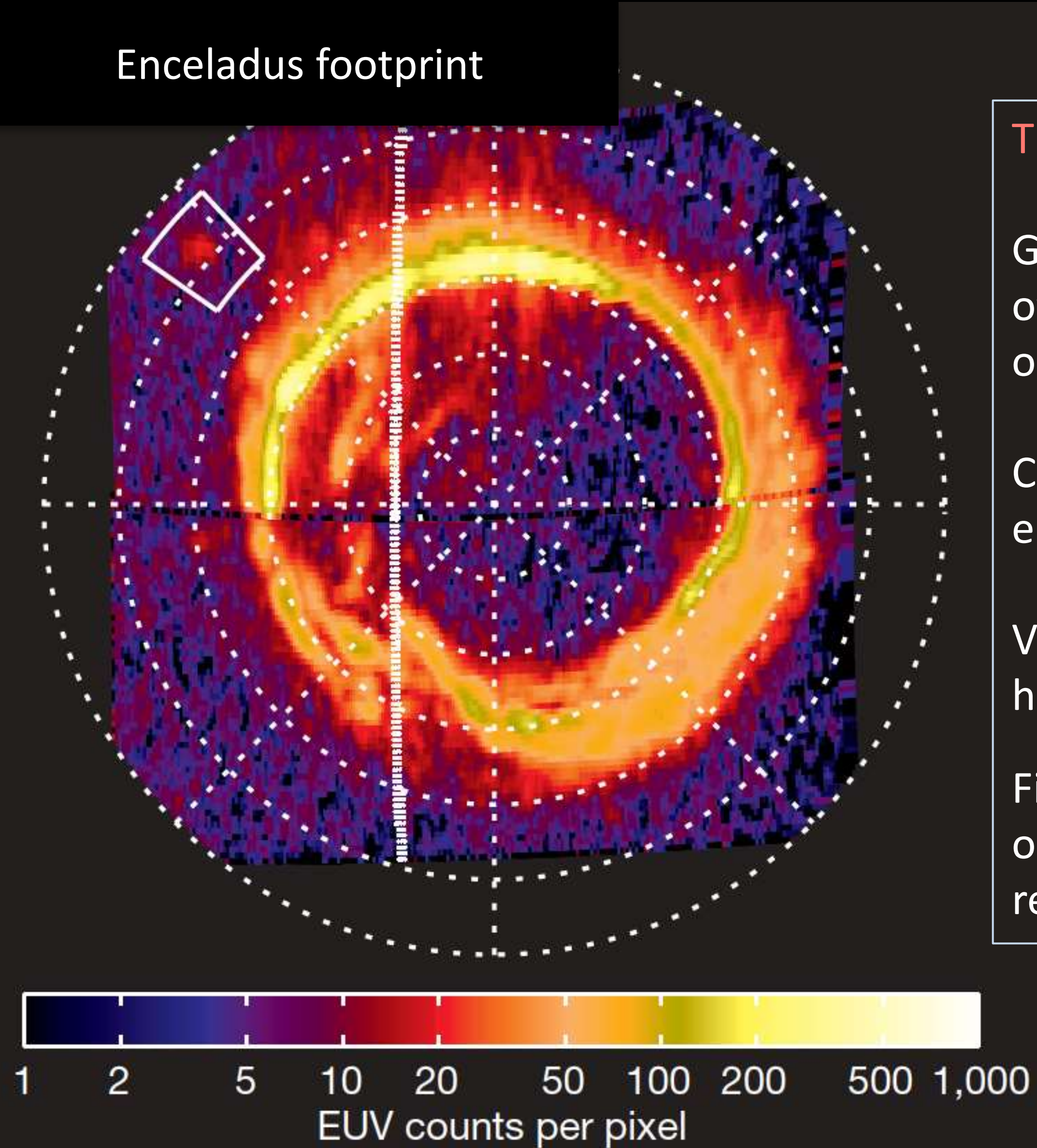

(Pryor et al., 2011)

The footprint :

Generally below detection threshold of about 1 kR (except in a few % of the observations)

Corresponds to precipitated electron energy of > 0.1 mW m^{-2} s^{-1}

Variable precipitation on timescale of a few hours

Field-aligned pitch angle distribution observed in the same magnetospheric region

Spatial scan of the north aurora (March 2011)

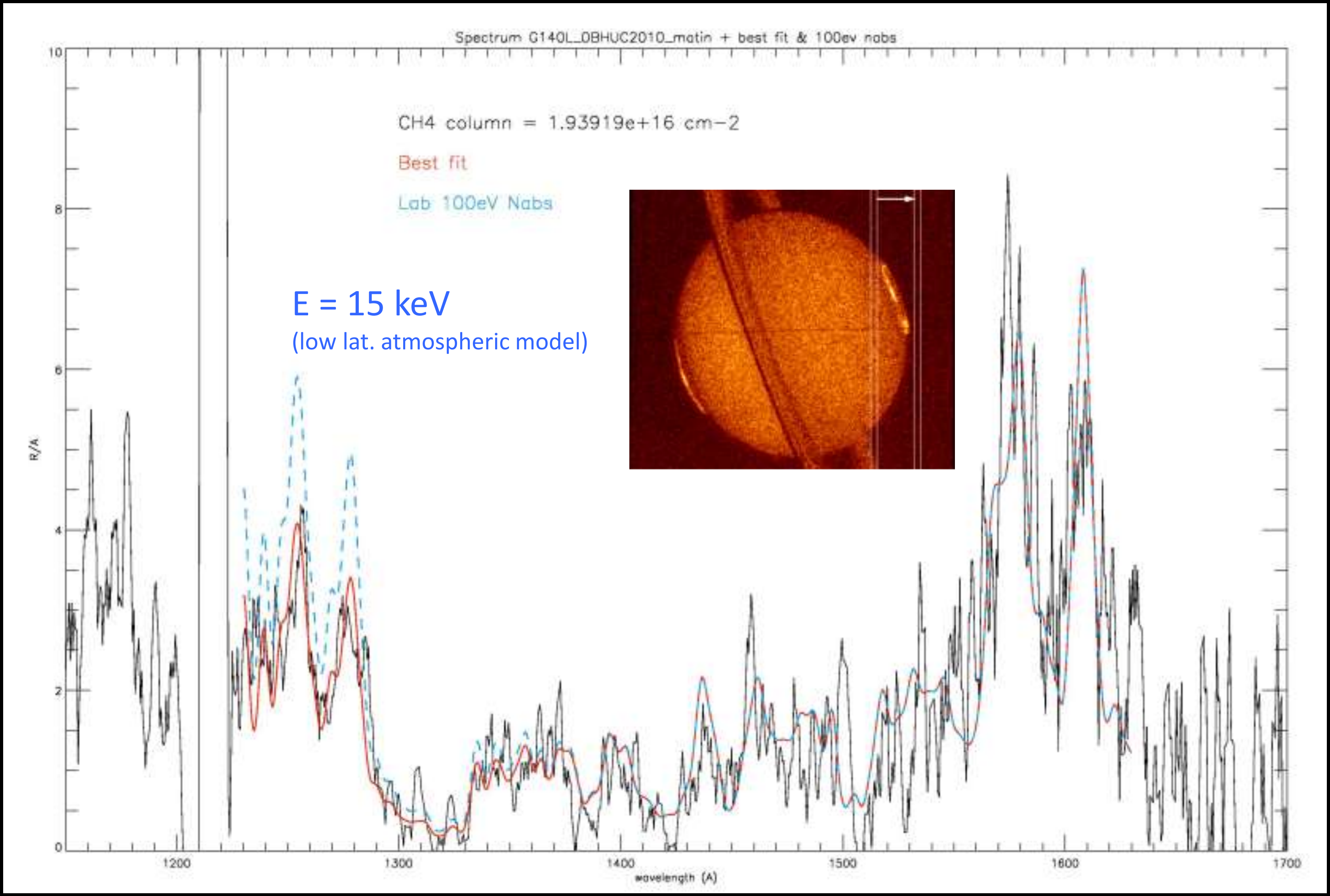

Work in progress

SUMMARY

- Several recent studies of the auroral morphology and energetics are concerned with structures other than the « main oval».
- The IR H_3^+ aurora is indirectly produced and its intensity depends on the amount of H_3^+ ions and the local temperature. It has the advantage to be observable from the ground
- Multipectral and time-dependent observations are adding important new clues
- The UVIS dataset provides an « improved view » of Saturn’s aurora with unprecedented visibility, sensitivity and resolution
- Improved magnetic mapping based on Cassini in-situ measurements footprint positions is now providing more accurate tools to locate the source of auroral precipitation

Continuous slowing down approximation

GÉRARD AND SINGH: JOVIAN AND SATURNIAN AURORAE

TABLE 3. Column Production Rates in Jovian Aurora

	Column Production Rates, kR						
	$\alpha = 0.1$ keV		$\alpha = 0.4$ keV		$\alpha = 2.0$ keV		$\alpha = 2.0$ keV
Emission	Case A	Case B	Case A	Case B	Case A	Case B	Pure H_2
Lyman bands	3.2 KR	112 R	1.4 KR	845 R	4.9 KR	3.1 KR	5.4 KR
Werner bands	3.0 KR	95 R	4.2 KR	750 R	4.6 KR	2.8 KR	5.2 KR
Hα	660 R	4.6 KR	280 R	2.5 KR	125 R	540 R	125 R
Hβ	50 R	260 R	28 R	147 R	20 R	36 R	20 R

H_2 emission in the Lyman (B-X) and Werner (C-X) bands: eff = **10.6 kR / mW m^{-2}** for electron precipitation with a mean energy exceeding a few hundred eV.

- UVS spectra taken on board Voyager indicate that almost all spectra show no indication of FUV absorption by hydrocarbons, implying that the bulk of the emission is produced above the homopause

- HST/STIS spectra taken near the central meridian (12:00 LT) indicate that the H2 emission is weakly absorbed, leading to an estimate of E ≈ 10 keV

- Recent analysis of Cassini/UVIS spectra confirms the Voyager results: absorption by hydrocarbons is generally not observed (Gustin, private comm.)

- FUSE observations of Saturn's EUV aurora set the altitude of the emerging emission to a level of H_2 = 3-6 x 10^{19} cm-^{2}, corresponding to a 0.1- 0.2 μbar level (Gustin et al, 2009)

2) Two-stream approximation (Waite et al., 1983, updated by Grodent et al., 2002)

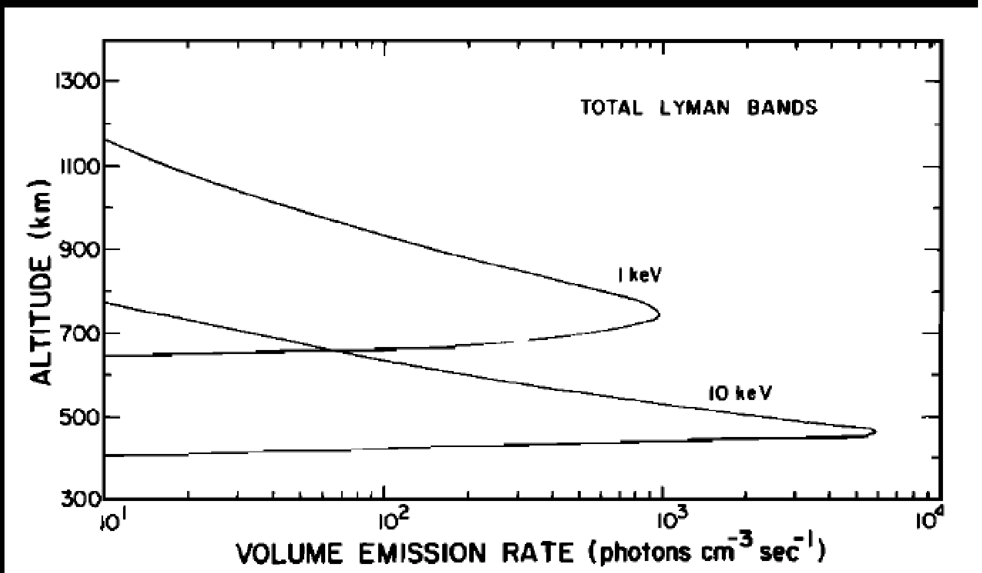

TABLE 5a. Energy Deposition Processes for the 10-keV Electron Beam: Unconverged Equatorial Atmosphere

	Column Rate cm^{-2} s^{-1}		Column Energy Efficiency, %
Energy input	6.25×10^{12} eV (10.0 ergs)		100.00
Backscattered	4.85×10^{10} eV		0.78
Lyman bands	5.14×10^{10}	92.3 kR	7.89 } 14.54
Werner bands	4.09×10^{10}		6.65
Lyman alpha	2.54×10^{10}	25.4 kR	4.23
H^+ (from H_2)	6.26×10^{9}		2.05
H_2^+	1.52×10^{11}		38.91
Vibration (direct)	9.62×10^{11}		8.31
Vibration (cascade)	4.10×10^{11}		3.32
H production (direct)	1.67×10^{11}		6.09
Electron heating	1.03×10^{11} eV		1.65
Neutral heating (direct)	6.91×10^{11} eV		11.06
H^+ (from H)	3.45×10^{8}		0.74
He^+	$\sim 1.30 \times 10^{8}$		~0.07
Miscellaneous (H, He, error, etc.)	. . .		8.32
			100.00

Eff = 9.2 kR/mW m^{-2}

Grodent et al. (2002) also obtained an efficiency of 10 kR/mW m^{-2}

3) Monte Carlo electron transport code

Recently, a Monte Carlo electron transport code in H_2-dominated atmospheres has been developed (short description in Gérard et al., 2009).

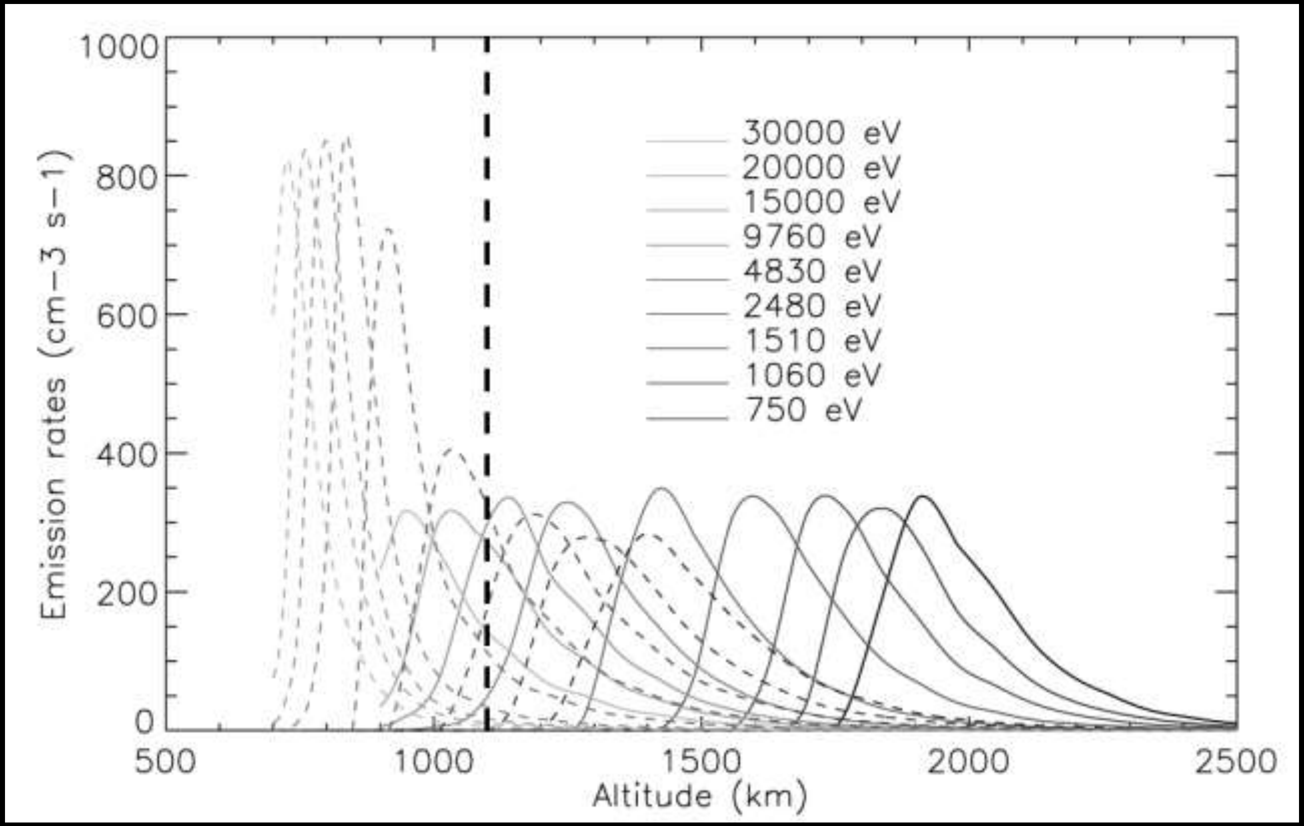

Altitude distribution of Saturn's aurora for various energies of the primary electrons

The results are again very close to those obtained with other methods.

The advantage of MC methods is that the direction of the electron beam is no longer fixed, but it varies following each collision in a stochastic manner.

Bifurcations of the main auroral ring at Saturn

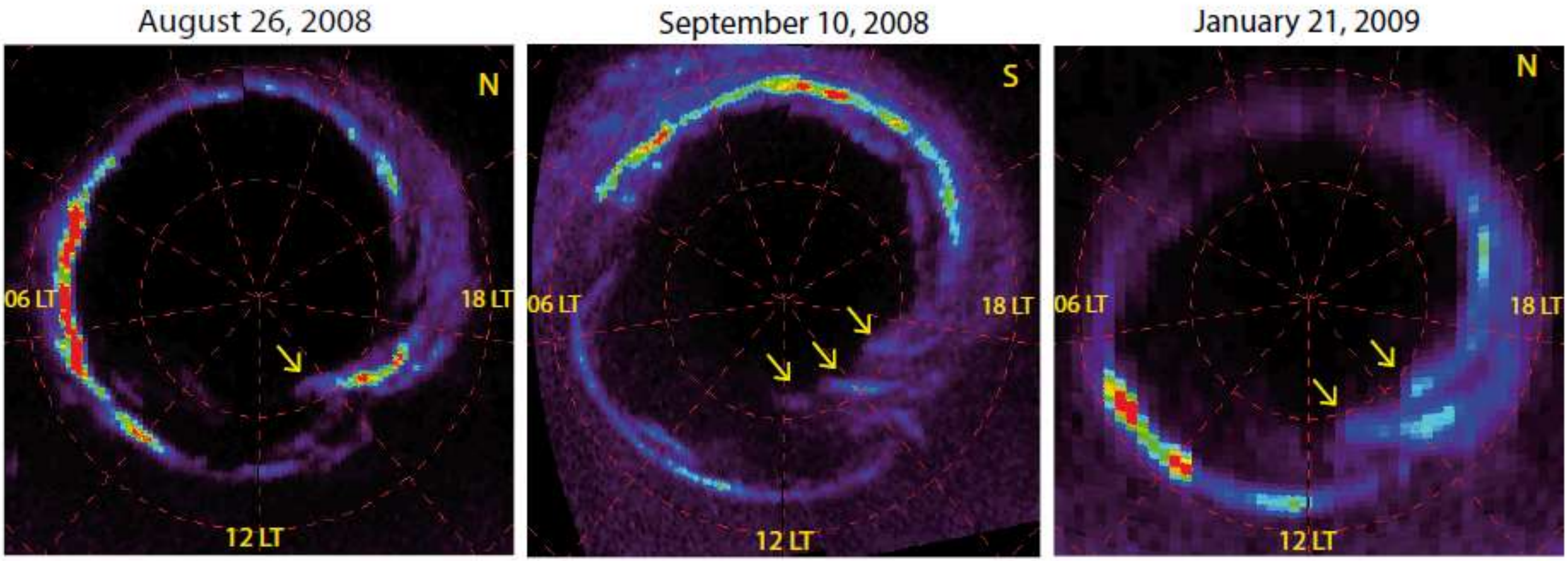

Preliminary statistics: Bifurcations are observed in 37% of the UVIS data analysed

Radioti et al., submitted

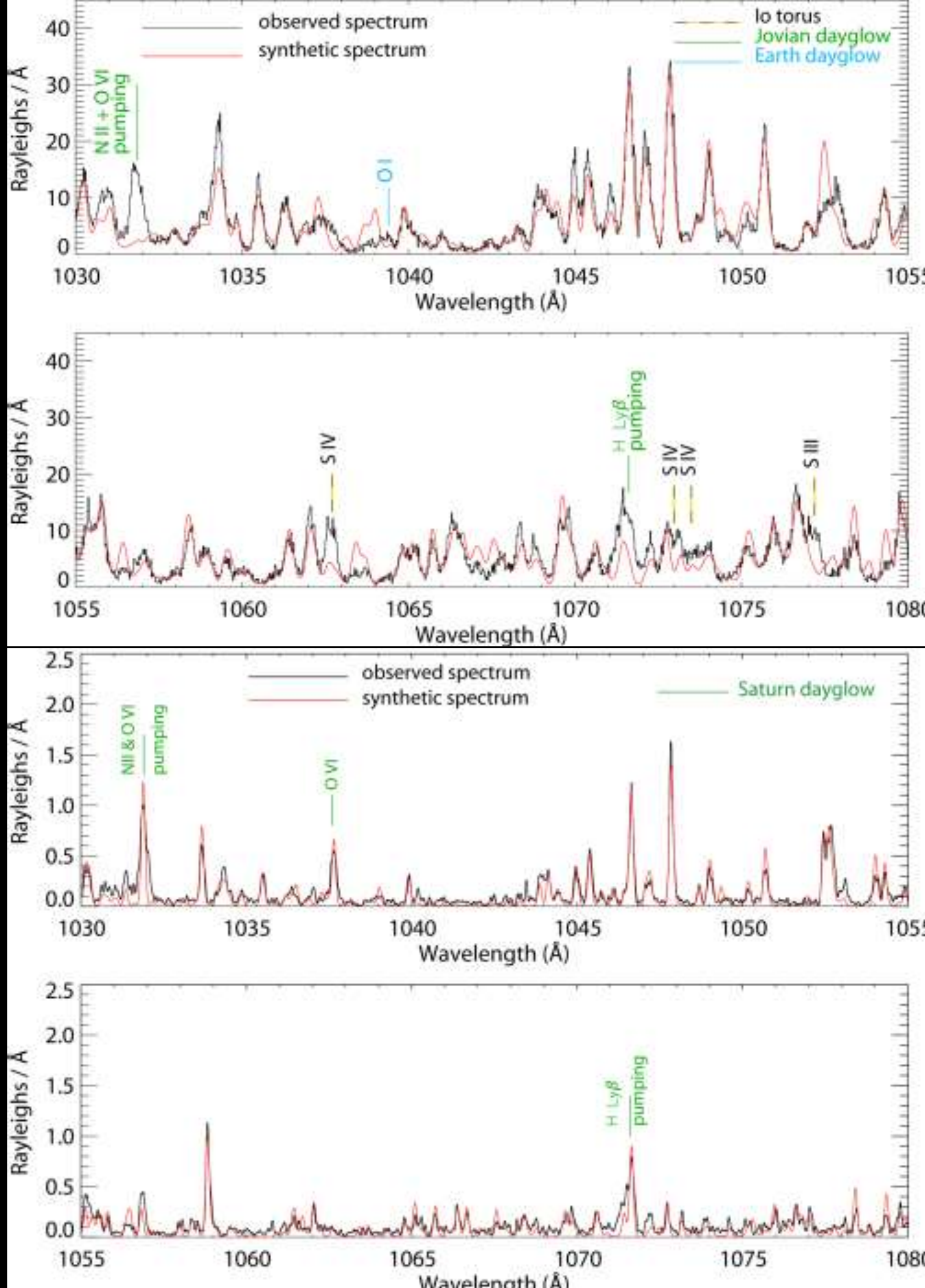

Jupiter

T(H_2): 800K

H_2 column:

1.5 x 10 ^{20} cm^{-2}

Saturn

T(H_2): 400K

H_2 column:

3 - <6 x 10^{19} cm^{-2}

The color ratio technique has been applied to Saturn's STIS and UVIS FUV spectra

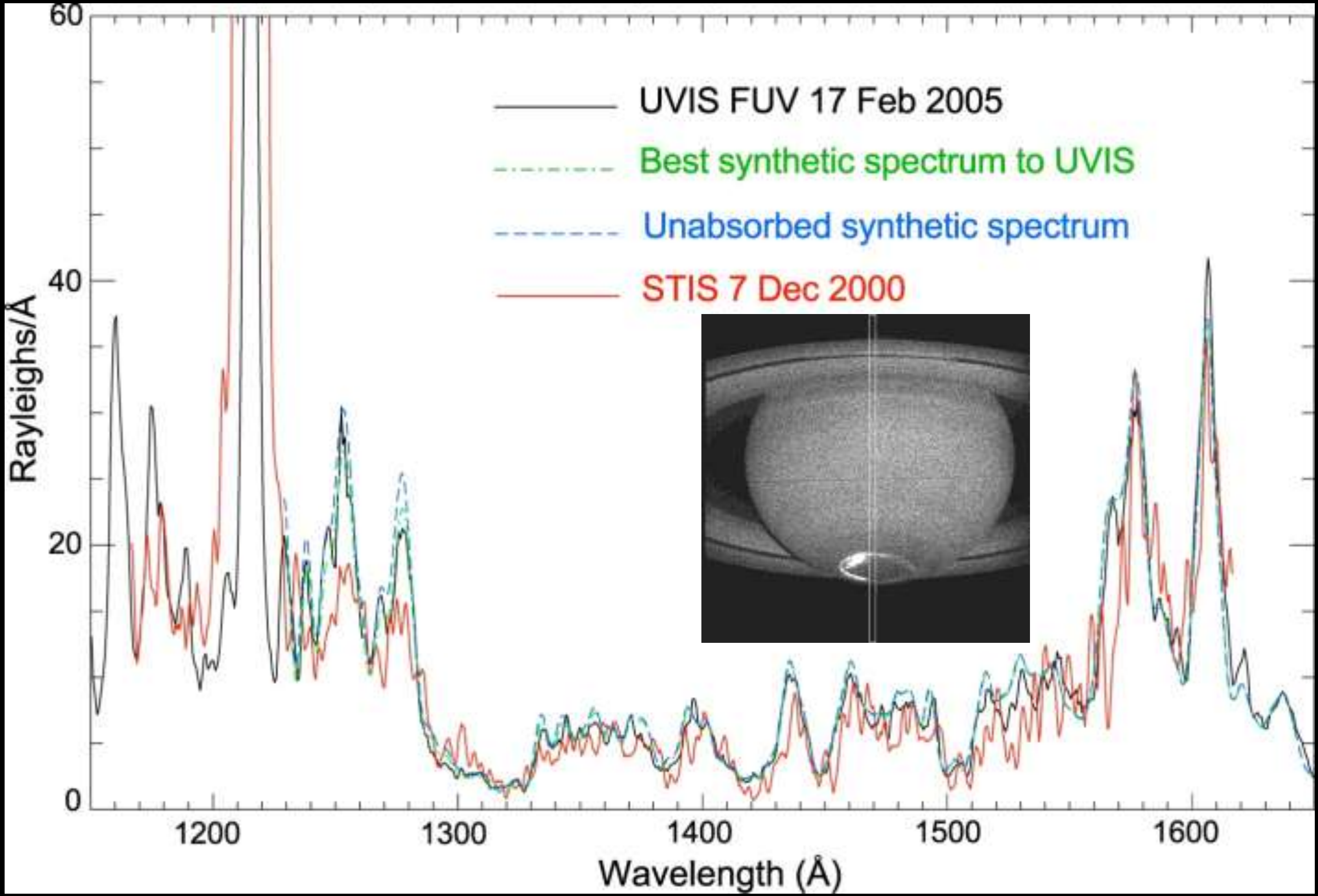

E ~10 keV

Gustin et al., 2010

Equatorward diffuse emissions (EDEs)

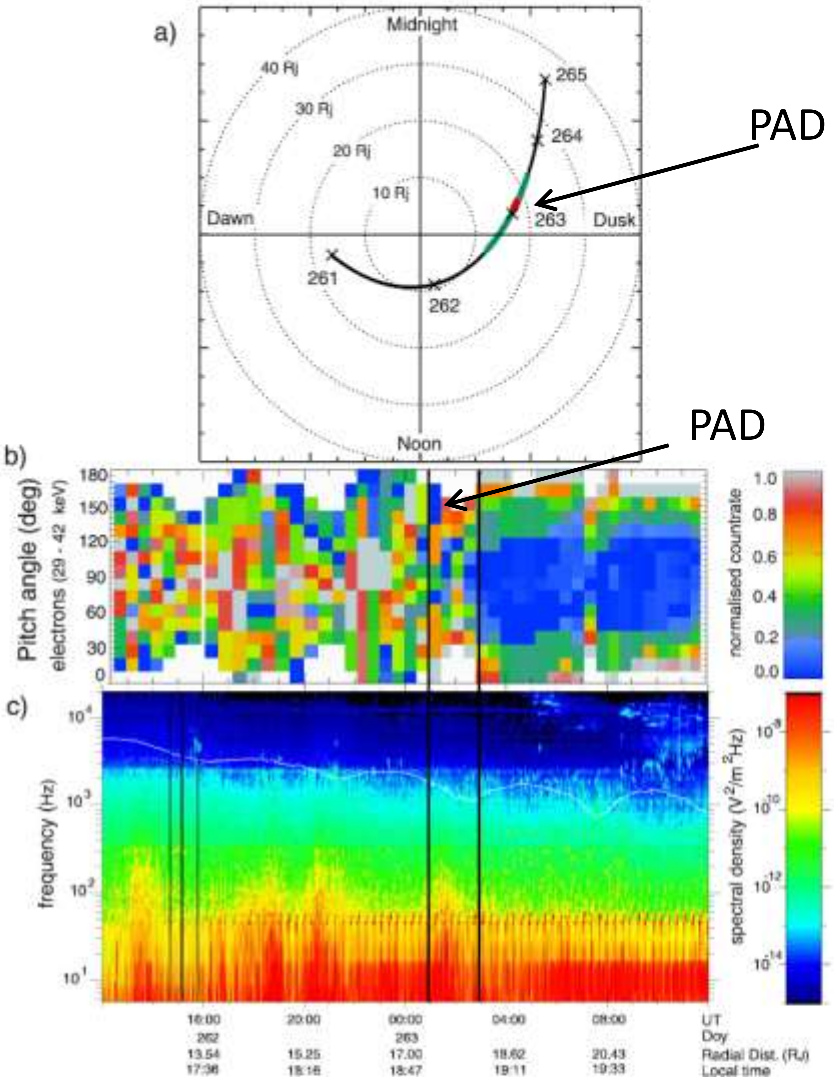

Based on quasi –simultaneous HST and Galileo wave and electron data the conditions for electron scattering by whistler mode waves have been tested and the energy flux precipitated in the ionosphere has been estimated

The derived precipitation energy flux and the observed auroral brightness indicates that the energy contained in the PAD boundary can account for the equatorward auroral emissions.

Radioti et al., 2009

Surface of the polar cap and open flux

Data analysis of a sequence over which bifurcations appear

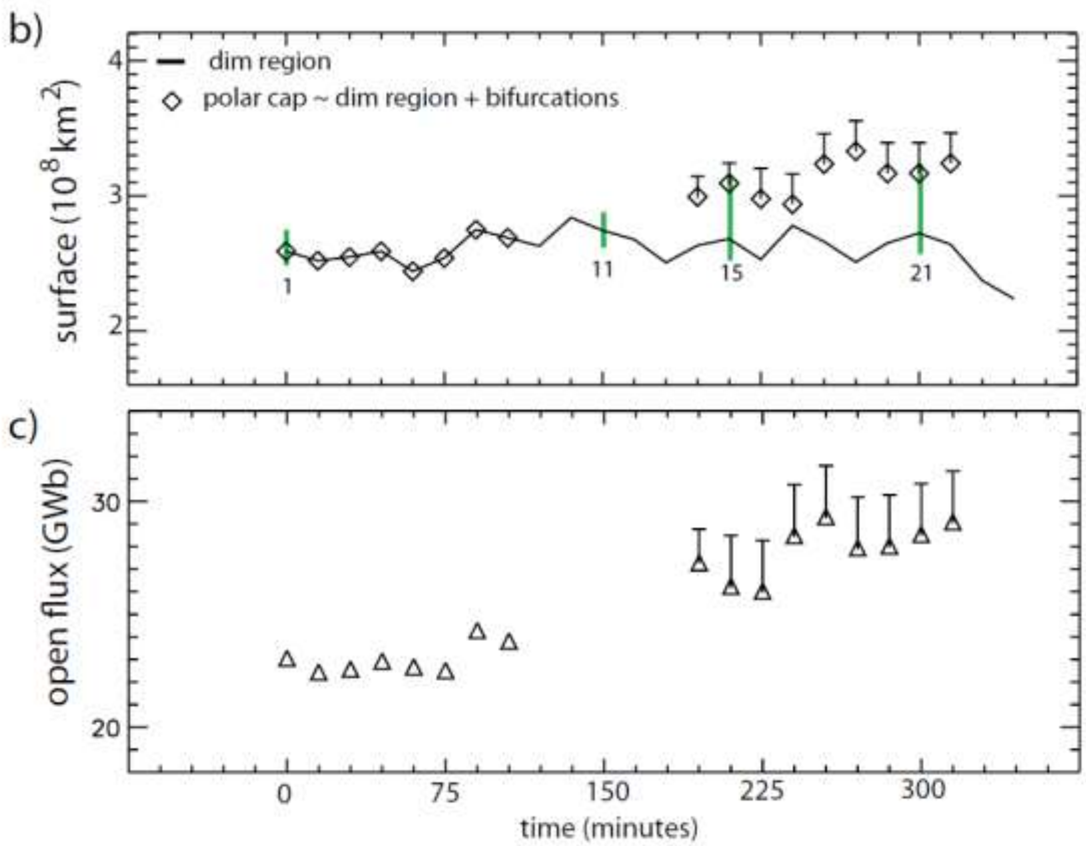

- Polar cap is expanding, expansion is equal to the area occupied by the bifurcations
- The open flux is increasing and the bifurcations represent the amount of newly open flux

Ionospheric signatures of reconnection events in the flank of the magnetopause

Radioti et al., submitted

Polar dawn spots and nightside spots

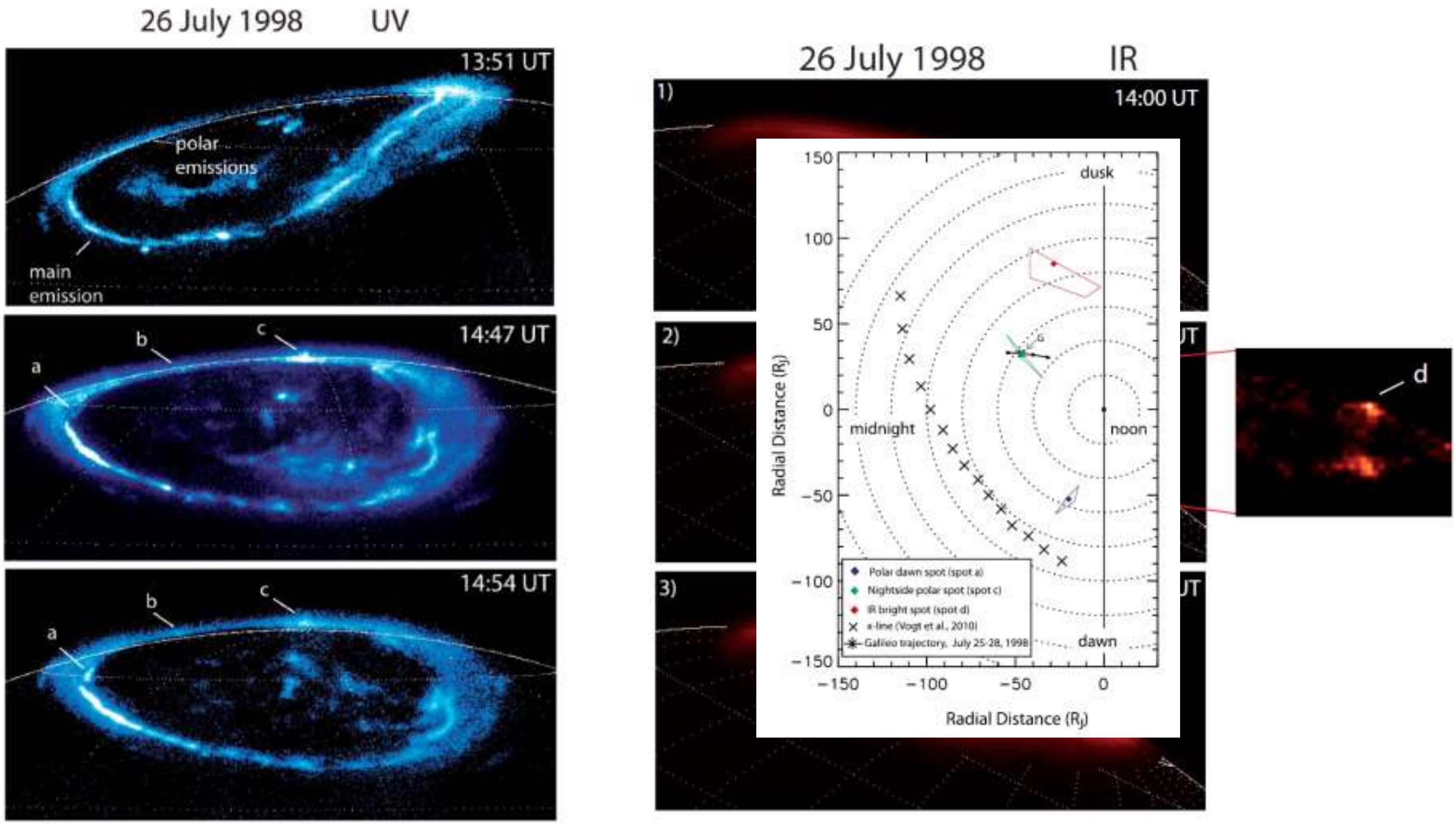

Near simultaneous UV and IR observations indicate that the transient nightside spots could have a common origin: tail reconnection as shown in previous studies for the UV spots (Radioti et al., 2010)

1-D spectral resolution in time-tag mode

North aurora

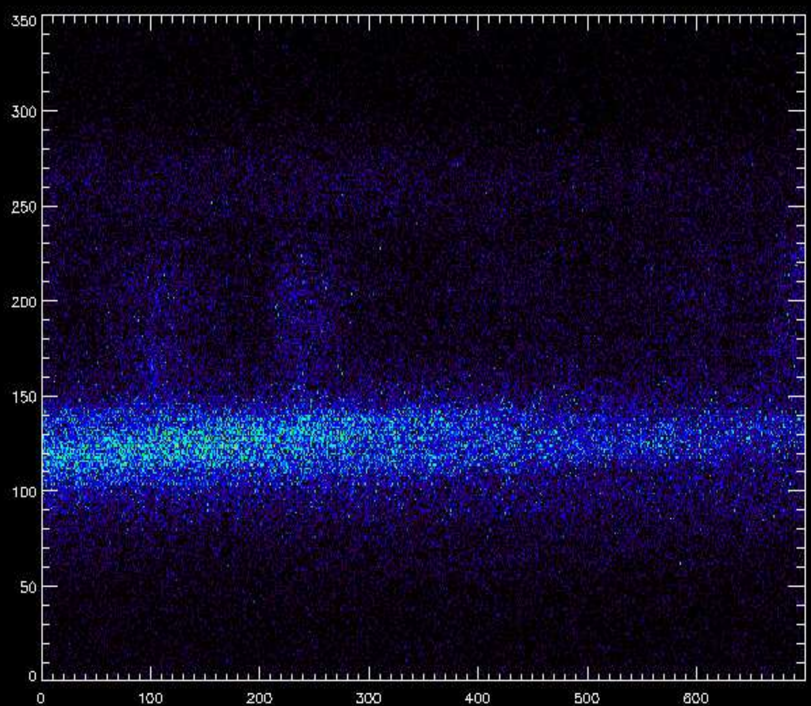

Time variation at high latitudes

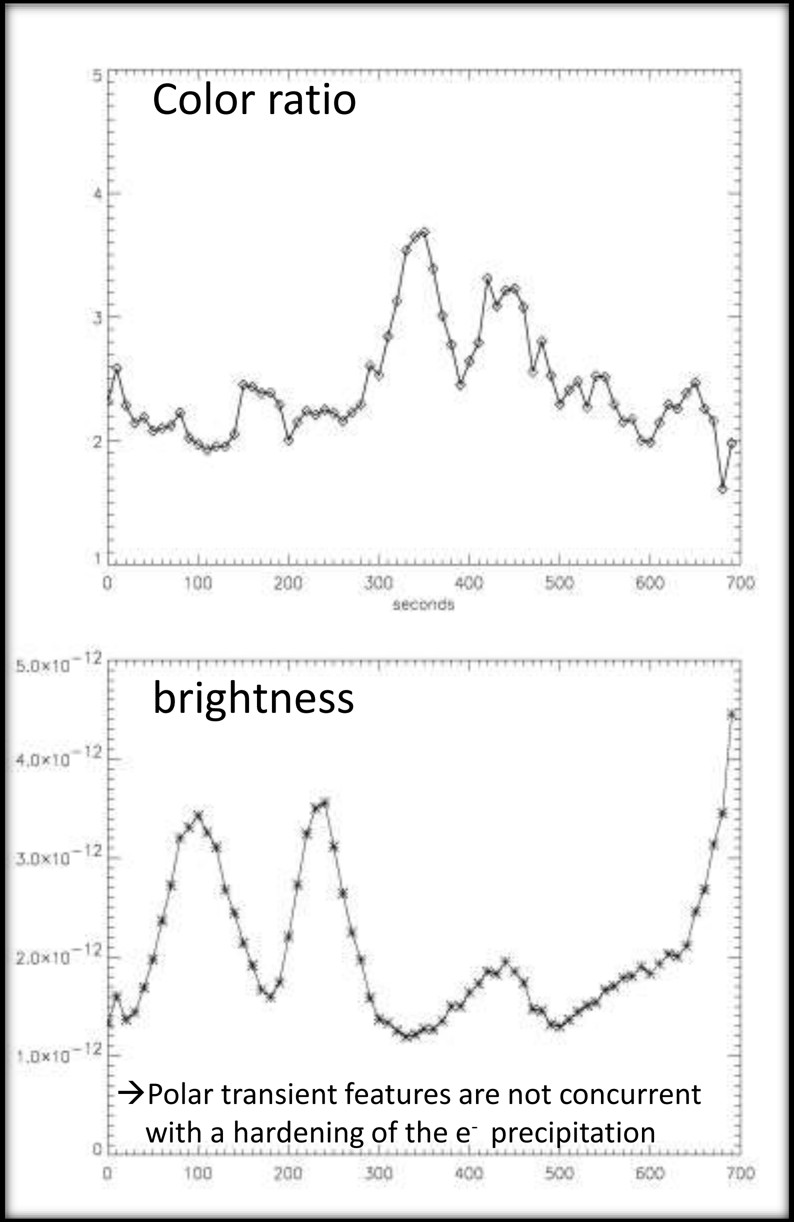

- The Jovian aurora shows different features in addition to the main oval: equatorward precipitation (wave-triggered precipitation), transient features field line reconnection as evidenced by ….), injections, quasi-periodic polar flares, etc …

- The satellite footprints are becoming bettter characterized in terms of morphology, size, temporal variations, etc …

- Saturn's auroral morphology is appearing more complex with Cassini UVIS high-latitude images. The structures suggest reconnection at the dayside magnetopause

- The changes in energy flux precipitated in Enceladus'footprint are not understood

The H_2 self-absorption method

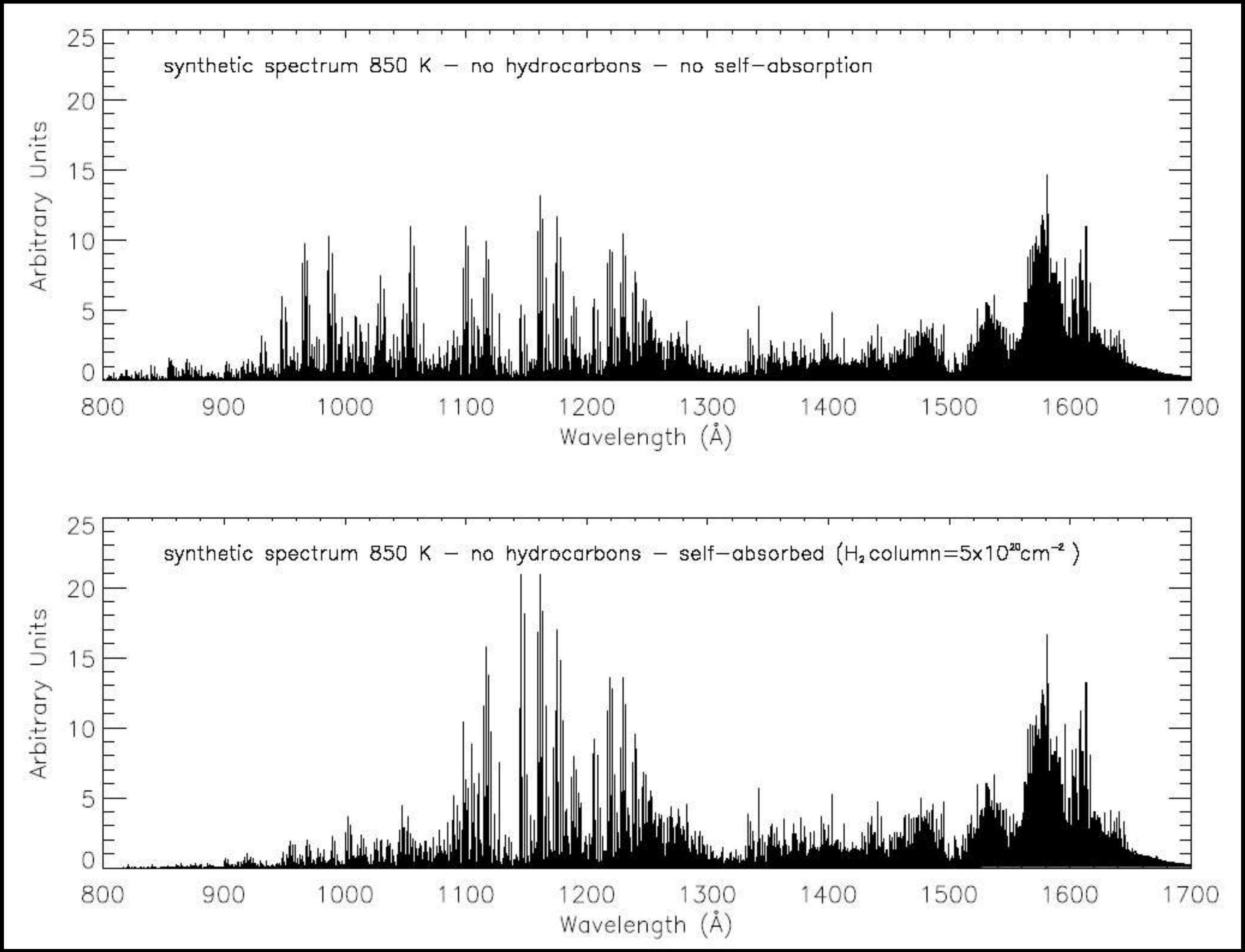

Gustin et al., 2005

Ganymede footprint brightness variations

- 5 hours – System III
  - Flapping of the current sheet
- 10-40 minutes
  - Related to injections?
- 100-seconds
  - Bursty reconnections at Ganymede?
  - Double layer generation?

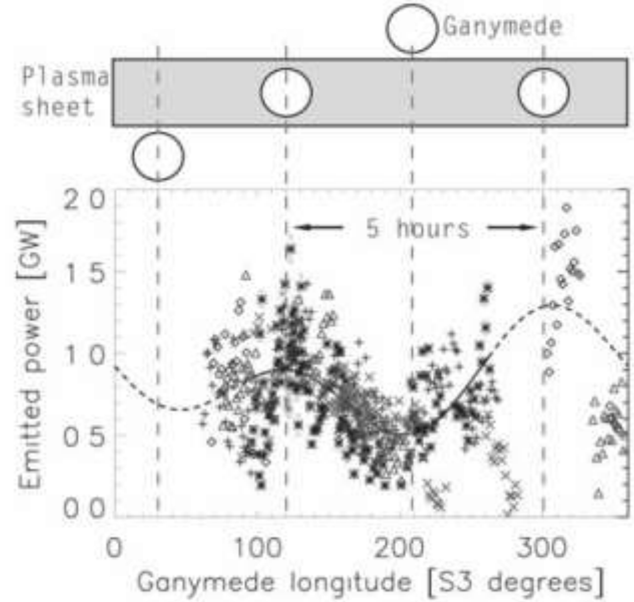

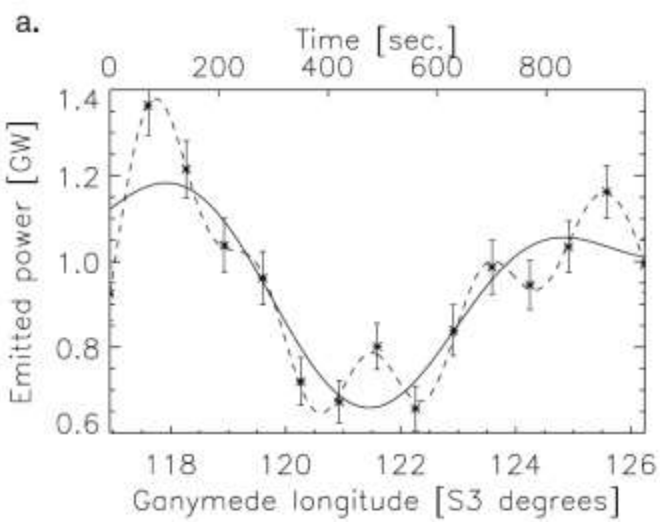

Grodent et al., 2009

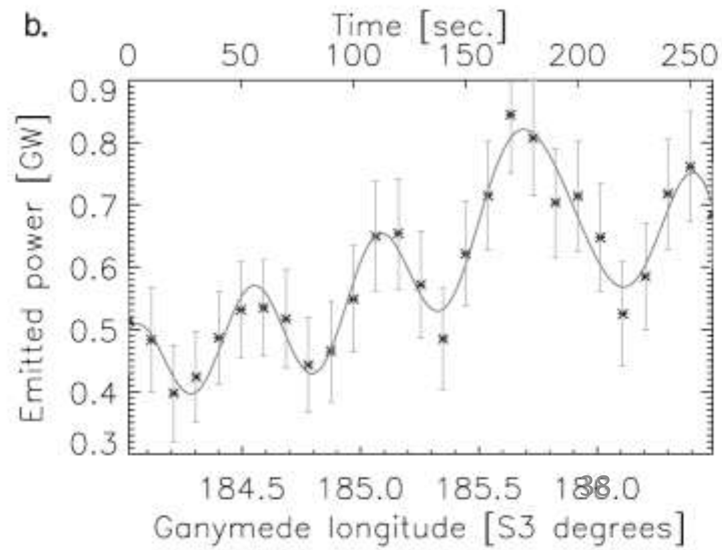

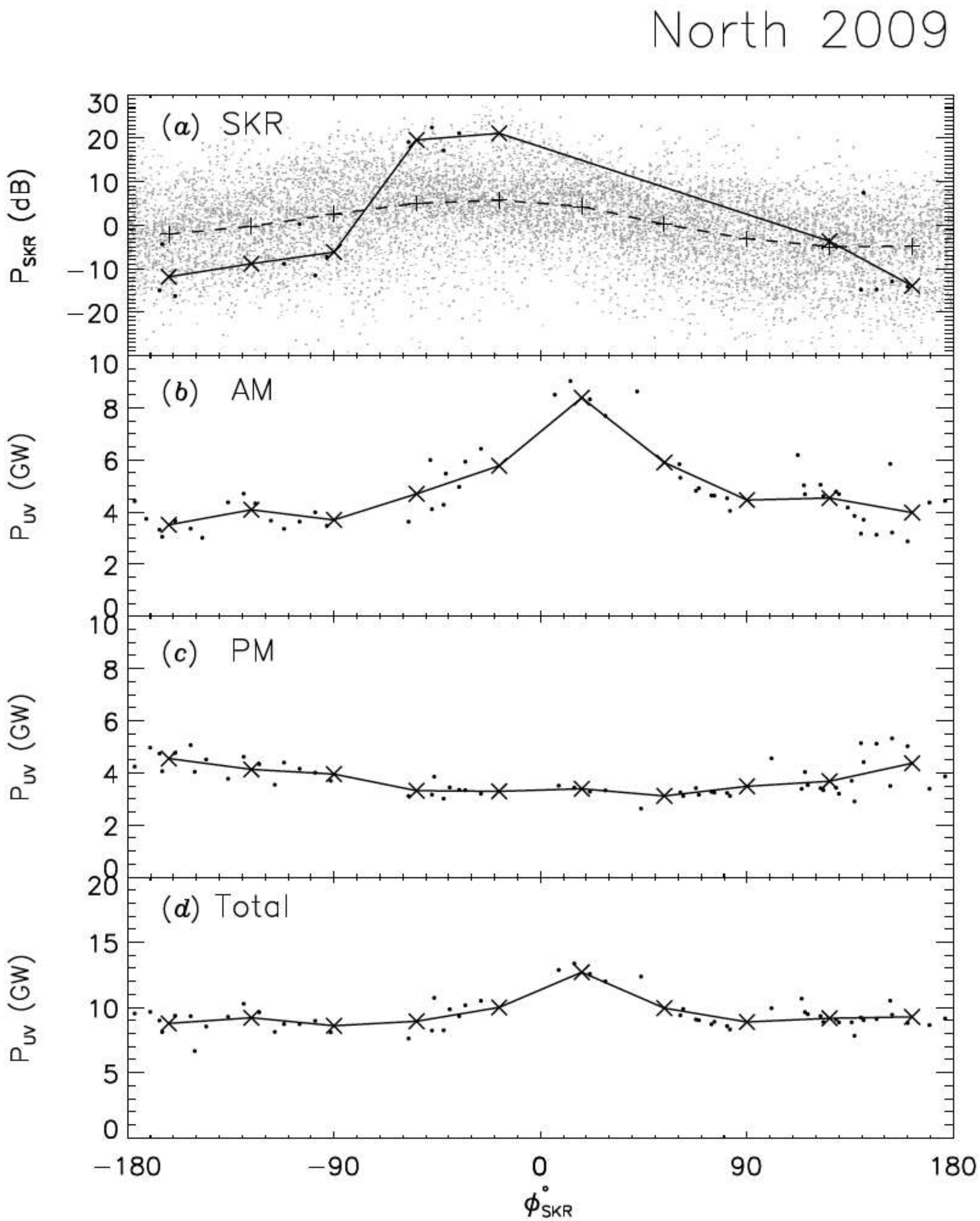

The auroral power emitted appears correlated with the SKR power, mainly in the morning sector.

The diurnal variation is about a factor of 3.

Nichols et al., 2010